

A NEW METHOD TO MEASURE VEHICLE PASS-BY NOISE IN A FINITE
DIMENSIONED SEMI-ANECHOIC ROOM

A THESIS SUBMITTED TO
THE GRADUATE SCHOOL OF NATURAL AND APPLIED SCIENCES
OF
MIDDLE EAST TECHNICAL UNIVERSITY

BY

ERSEN ARSLAN

IN PARTIAL FULFILLMENT OF THE REQUIREMENTS
FOR
THE DEGREE OF MASTER OF SCIENCE
IN
MECHANICAL ENGINEERING

SEPTEMBER 2010

Approval of the thesis:

**A NEW METHOD TO MEASURE VEHICLE PASS-BY NOISE IN A
FINITE DIMENSIONED SEMI-ANECHOIC ROOM**

submitted by **ERSEN ARSLAN** in partial fulfillment of the requirements for the degree of **Master of Science in Mechanical Engineering Department, Middle East Technical University by,**

Prof. Dr. Canan Özgen
Dean, Graduate School of **Natural and Applied Sciences**

Prof. Dr. Süha Oral
Head of Department, **Mechanical Engineering**

Prof. Dr. Mehmet Çalışkan
Supervisor, **Mechanical Engineering Dept., METU**

Examining Committee Members:

Prof. Dr. Y. Samim Ünlüsoy
Mechanical Engineering Dept., METU

Prof. Dr. Mehmet Çalışkan
Mechanical Engineering Dept., METU

Asst. Prof. Dr. Yiğit Yazıcıoğlu
Mechanical Engineering Dept., METU

Asst. Prof. Dr. Gökhan O. Özgen
Mechanical Engineering Dept., METU

Mechanical Engineer, M.Sc. Aytekin Özkan
T.O.F.A.Ş

Date: **14.09.2010**

I hereby declare that all the information in this document has been obtained and presented in accordance with academic rules and ethical conduct. I also declare that, as required by these rules and conduct, I have fully cited and referenced all material and results that are not original to this work.

Name, Last Name: Ersen ARSLAN

Signature :

ABSTRACT

A NEW METHOD TO MEASURE VEHICLE PASS-BY NOISE IN A FINITE DIMENSIONED SEMI-ANECHOIC ROOM

Arslan, Ersen

M. Sc., Department of Mechanical Engineering

Supervisor: Prof. Dr. Mehmet Çalışkan

September 2010, 103 pages

In this study, a method to predict vehicle pass-by noise in a finite dimensioned, semi-anechoic chamber with chassis dynamometer has been developed. Vehicle noise has been modeled as the summation of the individual contributions regarding the principal noise components, namely, engine including air intake, front tire and rear tire noises. This method employs wave propagation, Doppler shift, and time delay in the estimation of the sound pressure due to each component at points of interest specified by relevant standards. An acoustical simulation model has been developed in MaTLAB environment. The model has been applied on two different vehicles. Finally, the predicted sound pressure values are found to be in good agreement with the corresponding values acquired in outdoor measurements addressed in ISO 362 for vehicle pass-by noise measurement standard.

Keywords: Vehicle Pass-by Noise, Doppler Shift, Semi-Anechoic Chamber

ÖZ

SINIRLI BOYUTLARA SAHİP YARI-YANKISIZ AKUSTİK BİR ODA İÇERSİNDE ARAÇ GEÇİŞ GÜRÜLTÜSÜ ÖLÇÜMÜ İÇİN YÖNTEM GELİŞTİRİLMESİ

Arslan, Ersen

Yüksek Lisans, Makina Mühendisliği Bölümü

Tez Yöneticisi: Prof. Dr. Mehmet Çalışkan

Eylül 2010, 103 sayfa

Bu çalışmada, şasi dinamometresine sahip, sınırlı boyutlardaki, yarı-yankısız akustik bir oda içerisinde araç geçiş gürültüsünü öngörmeye imkan veren yeni bir yöntem geliştirilmiştir. Araç gürültüsü; temel gürültü kaynakları olan motor, ön tekerlek ve arka tekerleğin ayrı ayrı katkılarının toplamı olarak modellenmiştir. Her bir kaynağın standartta belirtilen mesafedeki gürültü değerlerinin hesaplanmasında; dalga yayılımı, Doppler Kayması ve zaman gecikmesi olguları kullanılmıştır. Benzetim modeli MaTLAB yazılımı içinde geliştirilmiştir ve iki farklı araç üstünde uygulanmıştır. Son olarak; öngörülen ses basıncı düzeyi değerleri, ISO 362'de tanımlanan ilgili dış mekan ölçümleriyle elde edilen değerlerle karşılaştırılmıştır ve uyumlu oldukları anlaşılmıştır.

Anahtar Kelimeler: Araç Geçiş Gürültüsü, Doppler Kayması, Yarı-Yankısız Akustik Oda

To my family

ACKNOWLEDGEMENTS

I wish to express my sincere appreciation to my supervisor Prof. Dr. Mehmet alıřkan for his guidance, advice, criticism, encouragements throughout the research and providing the opportunities to conduct the study.

Aytekin zkan, Can Bilir and Tarık Kck of TOFAŐ are greatly acknowledged for their help and offering facilities of NVH Department of TOFAŐ.

I would also like to thank my lover and my friends for their support.

This thesis study is supported by a grant from TOFAŐ through TUBİTAK, with project no 2008/270. TUBİTAK is also acknowledged.

And finally, I would like to thank my family for their continuous support and patience during every step of my education.

TABLE OF CONTENTS

ABSTRACT	iv
ÖZ.....	v
ACKNOWLEDGEMENTS.....	vii
TABLE OF CONTENTS.....	viii
LIST OF TABLES.....	xi
LIST OF FIGURES	xii
LIST OF SYMBOLS AND ABBREVIATIONS.....	xv
CHAPTERS	
1.INTRODUCTION	1
1.1 General.....	1
1.2 Motivation and Objective of the Present Study	3
1.3 Scope of the Thesis	4
2.REVIEW OF LITERATURE.....	5
2.1 General Review	5
2.2 Noise Sources on Road Vehicles.....	6
2.2.1 Power-train Noise.....	7
2.2.2 Intake and Exhaust Noise	8
2.2.3 Tire-Road Noise	9
2.2.4 Wind Noise	11

2.3 International Standards and Regulations.....	112
2.4 Prediction Methods of Vehicle Pass-by Noise Indoors	15
2.5 Beamforming and Nearfield Acoustic Holography	18
2.5.1 Beamforming	18
2.5.2 Nearfield Acoustic Holography (NAH)	20

3.THEORETICAL CONSIDERATIONS AND DEVELOPMENT OF THE PROPOSED METHOD..... 26

3.1 Time Records and Frequency Spectrum	26
3.2 Plane and Spherical Waves	27
3.2.1 Plane Waves:	27
3.2.2 Spherical Waves:.....	28
3.3 Sound Fields in Enclosed Space.....	29
3.4 Type of Sound Sources	31
3.4.1 Point Sources.....	32
3.4.2 Line Sources	33
3.5 Sound Emission From Moving Sources and Doppler Effect	35
3.6 Experimental Studies On Indoor Vehicle Pass-by Noise Measurements	41
3.6.1 Room and Dynanometer Requirements	42
3.6.2 Microphone Placement and Data Processing	44
3.6.3 Comparison of Indoor and Outdoor Pass-by Noise Measurement	45
3.7 General Overview of the Semi-anechoic Room	46
3.7.1 Acoustical Specifications of the Room.....	48
3.8 Noise Source Investigation of the Vehicle.....	49
3.8.1 Preliminary Test I (Engine + Tire + Exhaust).....	50
3.8.2 Preliminary Test II (Induced Exhaust Noise)	53
3.8.3 Preliminary Test III (Tire Noise)	55
3.9 Investigation of Vehicle Noise Propagation over Asphalt Ground	58
3.10 Simulation Model of Indoor Pass-by Noise.....	60

3.10.1 Microphone Positioning and Measurements	60
3.10.2 Sound Attenuation due to Distance	63
3.10.3 Simulation Model	64
4. EXPERIMENTAL AND SIMULATED RESULTS	67
4.1 Definition of the Measurements	67
4.2 Simulation Results and Comparison	71
4.2.1 Results	72
4.2.1.1 Results- Doblo	72
4.2.1.2 Results - Linea	74
4.2.2 Comparison of the Results	77
4.2.2.1 Comparison - Doblo	77
4.2.2.2 Comparison - Linea	79
5. SUMMARY AND CONCLUSIONS	81
REFERENCES	85
APPENDICES	92

LIST OF TABLES

TABLES

Table 2.1 Limiting SPL Values for Moving Vehicles [4].....	14
Table 3.1 Comparison of Outdoor and Indoor Pass-by Noise Measurements.....	46
Table 3.2 Acoustical performance of the semi-anechoic room in TOFAŞ.....	49
Table 3.3 Attenuation Values for corresponding Microphones for Outdoor.....	60
Table 4.1 Vehicle Specifications	67
Table 5.1 Predicted and Measured (Outdoor) Pass-by Noise Values	82

LIST OF FIGURES

FIGURES

Figure 2.1 Noise Sources on Road Vehicles	7
Figure 2.2 Typical Noise Spectrum for Light Vehicles [6]	8
Figure 2.3 Mechanisms of Intake and Exhaust Noise[13]	9
Figure 2.4 Tire-Road Noise Mechanisms.....	10
Figure 2.5 Typical sources of wind noise on Automobiles [6]	11
Figure 2.6 Test site dimensions [1].....	13
Figure 2.7 Plane waves hitting the microphones in the far field [30]	19
Figure 2.8 Illustration of Acoustic Holography[12]	21
Figure 3.1 Classification of Signals [53].....	26
Figure 3.2 Sound Fields in Enclosed Spaces [11].....	31
Figure 3.3 Illustration of Monopole Source	32
Figure 3.4 Illustration of Line Sources.....	34
Figure 3.5 Kinematics of a Moving Point Source.....	35
Figure 3.6 Moving Point Source (Subsonic Motion).....	40
Figure 3.7 Illustration of Measurements in a Semi-anechoic Room	42

Figure 3.8 Sound Absorption Mechanism inside the Acoustic Room	43
Figure 3.9 Limiting Values for inner Dimensions.....	44
Figure 3.10 Position of the rollers in the room	47
Figure 3.11 Test Setup	51
Figure 3.12 Frequency Spectrum for Second Gear between U=50km/h and U=61km/h	52
Figure 3.13 Frequency Spectrum for Third Gear between U=50km/h and U=57km/h	52
Figure 3.14 Mic-1 L_A Values for 2. and 3. Gear Tests.....	54
Figure 3.15 Mic-2 L_A Values for 2. and 3. Gear Tests.....	54
Figure 3.16 Mic-3 L_A Values for 2. and 3. Gear Tests.....	55
Figure 3.17 1/3 Octave Noise Spectrum at U=50km/h.....	56
Figure 3.18 1/3 Octave Noise Spectrum at U=55km/h.....	57
Figure 3.19 1/3 Octave Noise Spectrum at U=60km/h.....	57
Figure 3.20 Microphone Positions in Outdoor Test	59
Figure 3.21 Microphone Configurations	61
Figure 3.22 Illustration of Sound Pressure Attenuation due to Distance	63
Figure 3.23 Simulation Model for Indoor Pass-by Noise	64
Figure 4.1 Measurement Configuration for First Vehicle.....	68
Figure 4.2 Measurement Configuration for Second Vehicle.....	69
Figure 4.3 Throttle and Vehicle Speed Check (Valid Run)	71

Figure 4.4 L_A Values for Predicted Pass-by Noise, Engine Noise and Tire Noise for 2.Gear	72
Figure 4.5 Comparison of Predicted (Indoor) and Outdoor (ISO 362) Pass-by Noise Levels	73
Figure 4.6 L_A Values for Predicted Pass-by Noise, Engine Noise and Tire Noise for 3.Gear	73
Figure 4.7 Comparison of Predicted (Indoor) and Outdoor (ISO 362) Pass-by Noise Levels	74
Figure 4.8 L_A Values for Predicted Pass-by Noise, Engine Noise and Tire Noise for 2.Gear	75
Figure 4.9 Comparison of Predicted (Indoor) and Outdoor (ISO 362) Pass-by Noise Levels	75
Figure 4.10 L_A Values for Predicted Pass-by Noise, Engine Noise and Tire Noise for 3.Gear	76
Figure 4.11 Comparison of Predicted (Indoor) and Outdoor (ISO 362) Pass-by Noise Levels	76
Figure 4.12 Comparison of Pass-by Noise Levels (L_A) for Second Gear	78
Figure 4.13 Comparison of Pass-by Levels (L_A) for Third Gear	78
Figure 4.14 Comparison of Pass-by Noise Levels (L_A) for Second Gear	79
Figure 4.15 Comparison of Pass-by Levels (L_A) for Third Gear	80
Figure 5.1 Contributions of Tire Noise and Engine Noise (including air intake and exhaust) to the Overall Pass-by Noise Level	83

LIST OF SYMBOLS AND ABBREVIATIONS

A_{Dop}	Doppler Correction Coefficient
ASQ	Airborne Source Quantification
dB	Décibel
dBA	A-Weighted Sound (Pressure) Level in Decibels
M1,M2	Power-driven vehicles having at least four wheels and used for the carriage of passengers
NAH	Nearfield Acoustic Holography
TPA	Transfer Path Analysis
r	Distance from the Sound Source to the Receiver Point
r_{total}	Total Transmission Ratio
Δt	Sampling Period
ζ	Specific Normal Acoustic Impedance Time Shift
P	Sound Pressure Function
c	Speed of the sound
Q	Volume Velocity Function
I	Sound Intensity Function
W_o	Sound Power
L_w	Sound Power Level
L_p	Sound Pressure Level
L_A	A-weighted Sound Pressure Level
DI	Directivity Index
Q_i	Sound Strength of the Image Source

r_o	Plane Wave Reflection Coefficient
M	Mach Number
U_{vech}	Speed of the Sound Source
θ	Angle between the Direction of Motion and Position Vector
f	Frequency of the Original Signal
f_{k1}	Doppler Shifted Frequency
RPM	Revolution per Minute
U	Cruising Speed of the Vehicle
KHz	Kilohertz
f_c	Cut-off Frequency
R&D	Research and Development
t_c	Emission Time
t_r	Receiving Time
P_t	Circumference of the Tire
U_{vir}	Virtual Speed of the Vehicle
X_{vir}	Virtual Position of the Vehicle
SPL	Sound Pressure Level
NVH	Noise, Vibration and Harshness
FWD	Front Wheel Drive
RMSE	Root Mean Square Error

CHAPTER 1

INTRODUCTION

1.1 General

Over the last decades, emphasis on the applications for reducing the noise radiated from moving vehicles has increased in parallel to developing technology. Particularly, some countries and organizations adopted standards and directives regarding pass-by noise measurements due to environmental concerns and noise pollution. In these standards, the procedure for measurement the pass-by noise and limit values of the noise for specific type of road vehicles are described through outdoor measurements. However, difficulties involved in such measurements in outdoors, a controlled experimental procedure is needed. Researchers and engineers are now trying to implement new techniques for pass-by noise indoor measurement which has more advantages. In this thesis, methods which make it possible to measure vehicle pass-by noise in a finite dimensioned, semi-anechoic room with chassis dynamometer are investigated and a new method is developed for this purpose within the practical constraints posed by the manufacturer.

Vehicle pass-by noise is limited by International Standards (ISO 362, SAE J1470) and International Directives (European Union's 70/157/EC and 2007/34/EC). Along with European Union's environmental noise directive

(2002/49 EC), these legislations specify upper limits on sound levels produced by motor vehicles. Procedures about how to measure pass-by noise of a vehicle in outdoors are described in detail together with permissible sound levels of specific types of motor vehicles. More detailed information about these standards will be discussed in the following sections.

As addressed in the standards, pass-by noise measurement is to be done in outdoors to verify that a vehicle satisfies the permissible sound levels. However, outdoor measurement is affected by several factors like; weather conditions, road surface conditions and background noise. Also, it is difficult to fulfill the vehicle speed, throttle kick and down times procedures for which a talented driver is needed. On the other hand; provided that hemi-anechoic free field condition (principal condition of ISO 362) is satisfied within a semi-anechoic room equipped with a chassis dynamometer, vehicle pass-by noise measurements can be performed indoors, with good correlation to outdoor measurements. By making indoor measurement, the drawbacks of outdoor measurement are eliminated and manufacturers are able to predict the pass-by noise of a motor vehicle at the early stages of development.

In addition to free field condition, there are some other conditions that a semi-anechoic room has to satisfy so that the indoor vehicle pass-by noise measurement can be made. The vehicle is driven on a chassis dynamometer, such that its acceleration profile is similar to that is acquired in outdoors. The sound level of an operating chassis dynamometer is required to be at least 15 dBA lower than the total level being measured during tests. For example, in this thesis, the chassis dynamometer in the semi-anechoic room belonging to TOFAŞ with a sound pressure level of 48 dBA at 100km/h operating condition is used. Since pass-by noise levels are generally around 75 dBA , it meets the requirements for this study.

Prediction of the sound pressure level of a moving vehicle is a complex phenomenon. Doppler Effect which causes a shift in the frequency and amplitude of the signal as well as the sound wave propagation on reflective surfaces (earth surface) are the main topics that are to be considered. Another issue is that the vehicle is stationary and only its front or rear tires are operating in the case of indoor measurement. In contrast to the outdoor measurement, aerodynamic noise and contribution of either front or rear tires will be absent in indoor measurement. By using the fact that the speed of the vehicle changes between 50 km/h and 60 km/h in standard pass-by noise measurements, and the aerodynamic noise generated at these speeds are rather lower, the contribution of aerodynamic noise can be neglected in early stages of analysis.

The methods of prediction of sound pressure level at a specific point and applications in predicting the vehicle pass-by noise were reviewed in literature. Representing the noise sources of a vehicle as a monopole and assuming the engine is the main and dominant source, is a very common method in commercial software. Also, there are some examples of Near field Acoustic Holography (NAH) applications on vehicle pass-by noise indoor measurement as well as Transfer Path Analysis (TPA) and decoupling test methods.

1.2 Motivation and Objective of the Present Study

Regarding to ISO 362 standard, measurement area in the test site has a length of 20 m + length of vehicle (4 m to 6 m for passenger cars) and has a width of 15 m. It implies that the semi-anechoic room has to be at least, somewhat 26 m in length and 17 m in width. However, the semi-anechoic chamber belonging to TOFAŞ has limited inner dimensions and it does not fulfill the dimension requirements. Thus, a method to predict the

pass-by noise of a vehicle using the measurements done in a finite dimensioned, semi-anechoic chamber is needed.

The aim of this present study is to develop a new method for measuring the vehicle pass-by noise in a finite dimensioned, semi-anechoic chamber. This method needs to be compatible to ISO 362 and coherent with the corresponding vehicle pass-by noise outdoor measurement results.

1.3 Scope of the Thesis

The thesis is organized in five chapters. The following chapter provides the literature review related to noise sources regarding exterior vehicle noise phenomena. Also, International standards and regulations published for measuring vehicle pass-by noise are discussed. Finally, several indoor vehicle pass-by noise prediction methods are reviewed in literature.

In Chapter 3, theoretical considerations related to the pass-by noise prediction phenomena are given. Also, development of the proposed method is conducted using the information which is obtained through preliminary tests.

In Chapter 4, measurement setups for the two vehicles used in the experiments and simulations are presented. Simulated results obtained from the developed method are checked with the reference results of outdoor measurements. Also, the simulated results are compared with the results of commercial indoor vehicle pass-by noise software.

Finally, the thesis is concluded and future work of the proposed method is discussed in Chapter 5.

CHAPTER 2

REVIEW OF LITERATURE

2.1 General Review

The concept of measuring the pass-by noise of road vehicles was started to develop in the mid 1900s. It was in 1970 when the need for a pass-by noise measurement standard was first documented by ISO [1]. Since then, emphasis on the developments regarding the pass-by noise phenomena have increased and many engineers and scientists have studied the subject in detail [2-4].

If noise problems of road vehicles are categorized into two groups such that; interior noise problems and exterior noise problems; vehicle pass-by noise measurement is regarded to be an exterior noise problem. In exterior noise problems, the sound field is determined in an unbounded fluid domain. Comprehensive reviews and studies on the basic theory of sound waves can be found in literature [5-12].

Also, another classification can be made such that; sound sources related to engine speed "RPM" (Intake and Exhaust system Noise, Engine Noise) and those related to cruising speed "U" of the vehicle (Tire-road and Aerodynamic Noise).

Vehicle pass-by noise is due to many sound sources on the vehicle. According to the level of contributions, they can be classified under four primary titles. These are the power unit noise (engine noise), rolling noise (tire noise), intake system noise and exhaust system noise [6,13]. In addition, there are other sources like transmission noise, wind noise and exhaust shell noise which are of little effect on the overall pass-by level[6,14]. There are many studies in literature which investigate the characteristics of the sound sources of road vehicles and show the contributions of each sound sources to the overall measured level with test-based information[15-20].To reduce the pass-by noise of the vehicle, one must find the dominant noise source and identify it. With the help of advanced technology in data acquisition process, source identification becomes more and more important to automobile manufacturers.

2.2 Noise Sources on Road Vehicles

In this section, only the sound sources regarding exterior noise phenomena will be discussed. These are power-train noise, intake and exhaust noise, tire noise and wind noise.

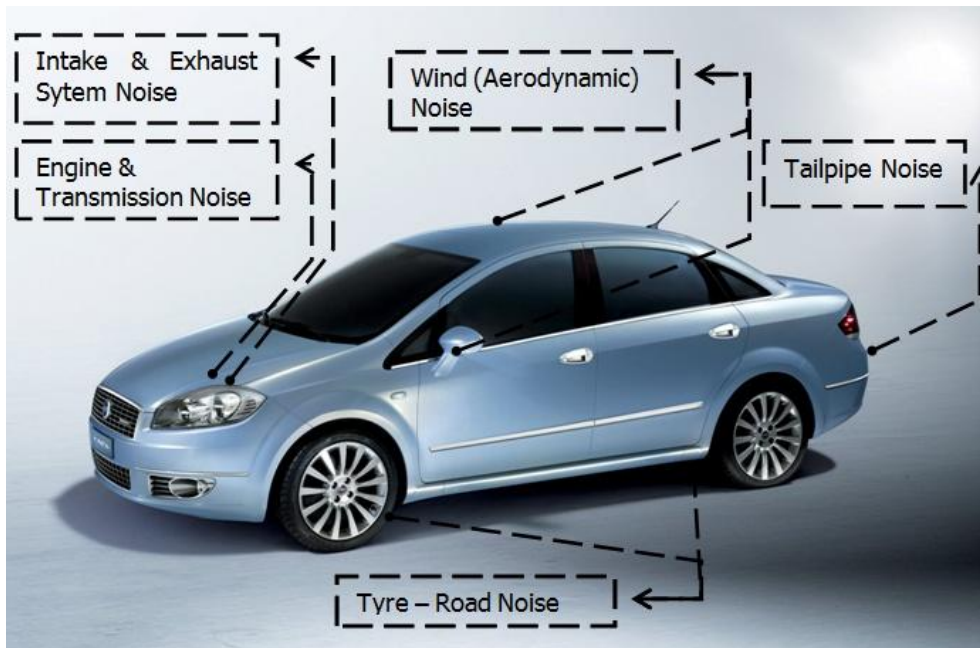


Figure 2.1 Noise Sources on Road Vehicles

2.2.1 Power-train Noise

The term “Power-train” is used here only to include engine and transmission components of a road vehicle. In this section only the general noise mechanisms regarding a traditionally reciprocating, four-stroke, internal combustion engines will be investigated.

Power-train noise sources are indeed numerous such as valve gear, drive system, oil pump, alternator, cooling fan, turbo charger, diesel injection system, etc. However, only noise emitted from the combustion of the fuel in the cylinders and the operation of the piston cranks can be regarded as a primary noise sources. These are dominantly controlled by the speed of the engine and thus, sound signals coming from them can be considered to be non-stationary from signal classification stand point (see Section 3.1). Also, the shape and the size of the engine are the factors that are relevant with characteristic noise of the engine. According to the studies

regarding the engine noise, noise spectrum of power-train components lie around 1-2 kHz [6].

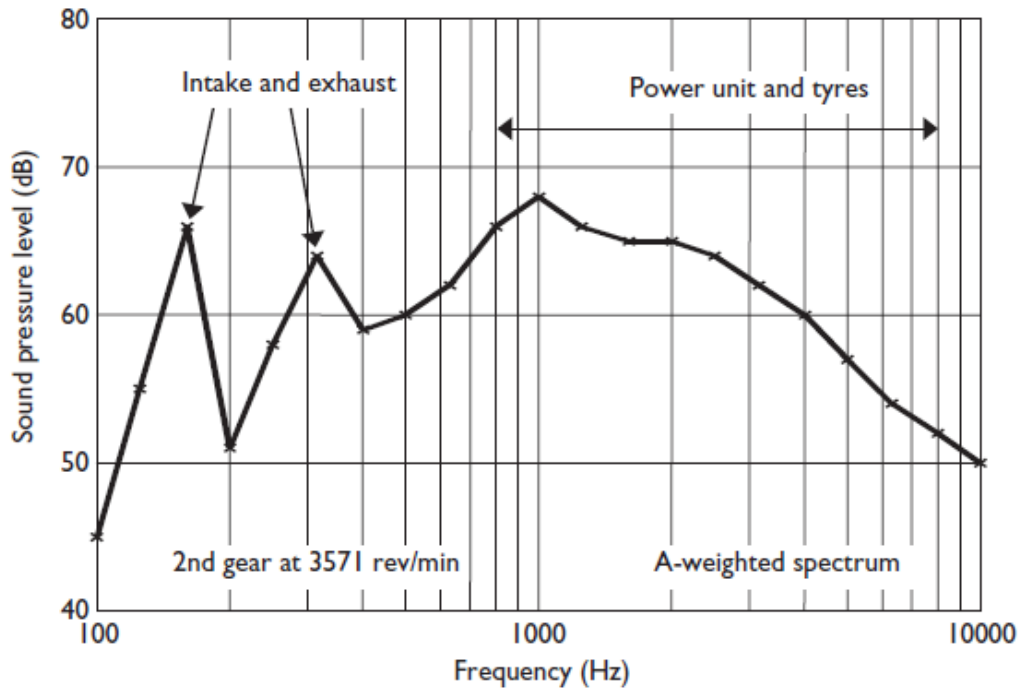


Figure 2.2 Typical Noise Spectrum for Light Vehicles [6]

2.2.2 Intake and Exhaust Noise

Noise generated by both intake system and exhaust system is similar. Generally, two mechanisms which are both regarded as air-borne noise are dominant on the overall sound level with respect to the structure-borne [13]. First one of them is due to the instantaneous change in the mass flow of the fast moving air through the valves. These fluctuations then propagate to the system's inlet orifice where they radiate as noise. Similarly, in the case of the exhaust flow, hot air coming from the combustion process in the cylinders exits through the valves to the exhaust tailpipe and generates

noise. The second mechanism is due to the motion of the fast moving air through the intake and exhaust systems.

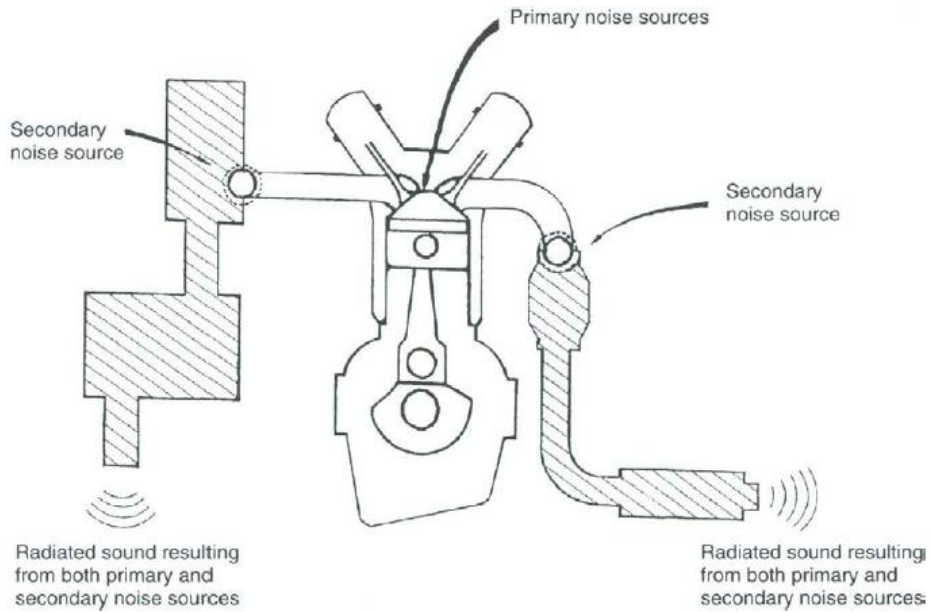


Figure 2.3 Mechanisms of Intake and Exhaust Noise[13]

2.2.3 Tire-Road Noise

Tire-road noise is one of the major sources of vehicle pass-by noise. Based on their generation and radiation, tire-road noise phenomena can be divided in two groups. In the first group, impact and slip-adhesion noise are regarded as structure-borne noise, while air pumping is taken as air-borne noise in the second group [6, 13, 55, 56].

In air pumping mechanism, when the contact patch of a rolling tire comes into effect with the road surface, the passages and grooves in the tire are compressed and as a result, the air in these passages is squeezed out. Inversely, when the contact patch leaves the road surface, the passages and

the grooves return to their original dimensions which make the air to be sucked in. Thus, air-borne noise with a spectral content ranging from 500 - 3000 Hz is generated [55].

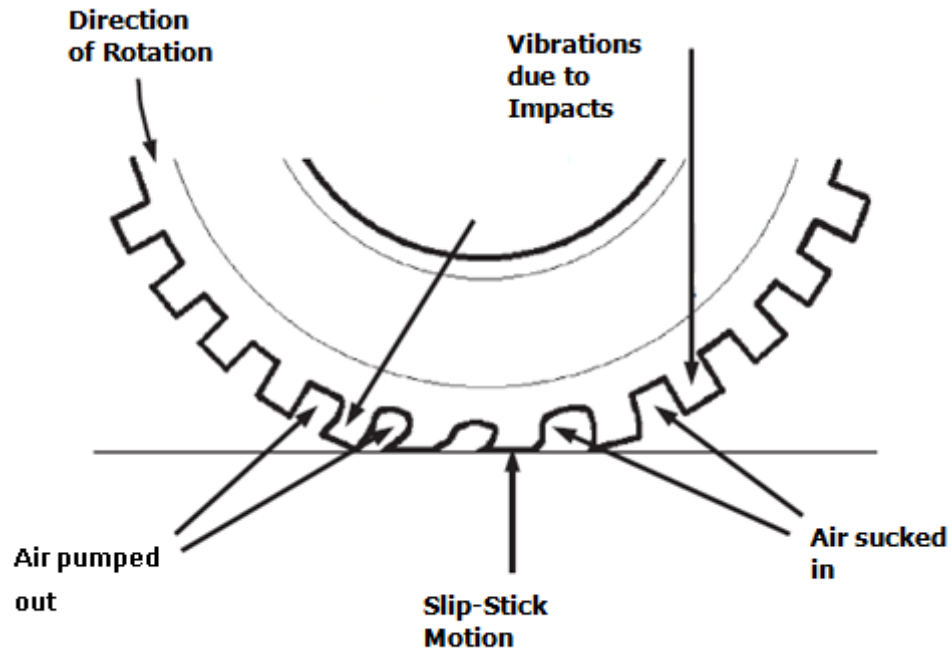


Figure 2.4 Tire-Road Noise Mechanisms

Impact noise mechanism essentially consists of the excitation of tire tread as the tread hits the road surface which is dominantly controlled by road surface roughness. At high speeds, when this mechanism is rapid, both radial and tangential vibration modes of the tire are excited. The frequency range of this type of noise is to be effective below 1 kHz due to low pass band filter feature of the tire [55].

Another noise mechanism is caused by friction forces between the tire and the road surface. Especially, when the vehicle is accelerated or decelerated, due to the tangential forces between the tire and the road surface, the action of slipping and sticking happens. Thus, vibration and noise is generated related to the slip velocity of the tread. Also, the contact

between the tire (tread) and the road surface causes adhesion forces. When the tread leaves the ground surface, both sound and vibration occurs.

2.2.4 Wind Noise

Among other types of noise sources on automobiles, wind noise is highly dependent on the cruising speed “U” of the vehicle. Especially in the high speed region where the cruising speed is over 100 km/h, aerodynamic noise becomes more important issue that others because it is proportional to the order of sixth power of the vehicle cruising speed [6,13,57].

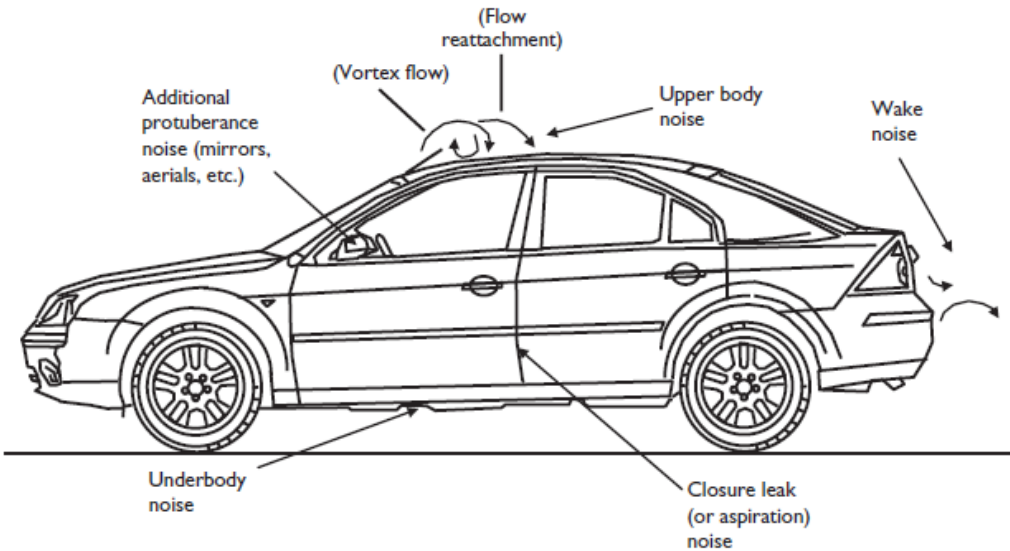


Figure 2.5 Typical sources of wind noise on Automobiles [6]

The wind noise generation is dependent on many factors like the exterior shape of the vehicle and cruising speed (Fig 2.5). However; in pass-by noise measurements where cruising speed is around 50-60 km/h, the contribution of wind noise to the overall sound level is very low [6]. Thus,

the effect of wind noise is neglected in the indoor pass-by noise prediction studies.

2.3 International Standards and Regulations

There are two standards describing the procedure for measuring the pass-by noise of a vehicle. One of them was issued out by ISO (the International Organization for Standardization) [1]. The related standard for pass-by noise, ISO 362, gives very detailed information about the measurement setup and requirements. The other standard which is SAE J1470, is commonly used in the U.S. In this study ISO 362 was taken as a reference standard. Hence, it is focused on and explained in detail.

In ISO 362, "the procedure provides a measure of the sound pressure level from vehicles under controlled and repeatable conditions. The definitions have been made according to the needs of vehicle categories. In cases of vehicles other than very heavy trucks and buses, the working group found that attempts to conduct a partial load test as in actual use resulted in considerable run-to-run variability that significantly interfered with the repeatability and reproducibility of the test cycle. Therefore, two primary operating conditions (i.e. a wide open-throttle acceleration phase, and a constant speed phase) were used to guarantee simplicity. The combination was found to be equivalent to the partial throttle and partial power (engine load) actually used." [1]

The standard has a detailed content explaining the procedure step by step. Firstly, terms and definitions associated with vehicle are described. It categorizes the vehicles regarding their mass and number of wheels. In the instrumentation subtitle, requirements for the instruments which will be used in the test are revealed and limits for the engine and vehicle speeds are pointed out. The test site specifications are described with the test site

was published in 2007 is presented with new amendments highlighted in Appendix A.

Table 2.1 Limiting SPL Values for Moving Vehicles [4]

Vehicle categories	Values expressed in dB (A) (decibels (A))
5.2.2.1.1. Vehicles intended for the carriage of passengers, and comprising not more than nine seats including the driver's seat	74
5.2.2.1.2. Vehicles intended for the carriage of passengers and equipped with more than nine seats, including the driver's seat; and having a maximum permissible mass of more than 3,5 tonnes and:	
5.2.2.1.2.1. — with an engine power of less than 150 kW	78
5.2.2.1.2.2. — with an engine power of not less than 150 kW	80
5.2.2.1.3. Vehicles intended for the carriage of passengers and equipped with more than nine seats including the driver's seat; vehicles intended for the carriage of goods:	
5.2.2.1.3.1. — with a maximum permissible mass not exceeding 2 tonnes	76
5.2.2.1.3.2. — with a maximum permissible mass exceeding 2 tonnes but not exceeding 3,5 tonnes	77
5.2.2.1.4. Vehicles intended for the carriage of goods and having a maximum permissible mass exceeding 3,5 tonnes:	
5.2.2.1.4.1. — with an engine power of less than 75 kW	77
5.2.2.1.4.2. — with an engine power of not less than 75 kW but less than 150 kW	78
5.2.2.1.4.3. — with an engine power of not less than 150 kW	80

Automobile manufacturers also should pay great attention to the directives which vehicles have to satisfy so that they can market them in respective countries. The measurement procedure and requirements are described in Directives 70/157/EEC and 2007/34/EC of the European Union relating to the permissible sound level of motor vehicles. In Annex I of the Directive 70/157/EEC, definitions of the procedure for measuring the sound level of the vehicle are made. The sound emitted by the type of vehicle submitted for EEC type-approval must be measured in accordance with each

of the two methods; in the case of moving vehicles and in the case of stationary vehicles, respectively. The limits of sound level of the moving vehicles are stated, and those limits shall not be exceeded in order to comply with the directives.

2.4 Prediction Methods of Vehicle Pass-by Noise Indoors

Several studies about prediction of vehicle pass-by noise can be found in literature. Especially, Korean and American researchers have dealt with this subject and decent methods have been proposed. Lately, European researchers have also put significant efforts on vehicle pass-by noise prediction studies. Below, five different pass-by noise prediction studies are discussed.

Kim, Yoo, Kim and Zwanzig developed a method for prediction of vehicle pass-by noise using indoor measurements [17]. Doppler Effect of moving vehicle as in the case real operating conditions is taken into account as frequency shift and time delay. Decoupling techniques are implemented to investigate principal sound sources on the vehicle and noise propagation characteristics are tried to be approached by using the measurements made in the near field based on formerly acquired test results. In these measurements, virtual sound strengths of principal sound sources (engine, tire, and tailpipe) are calculated, and along with the Doppler Effect, wave propagation is carried out for estimating the sound pressure levels of each principal sound source. By summing up the contributions for each source, an overall level of pass-by noise of a vehicle is obtained.

In the scope of the research program which was funded by European Commission, studies about prediction and simulation of pass-by noise were conducted [21]. Advanced software which is able to give results like sound pressure with regard to time, octave band analysis and time evolution of the

pressure level was developed. The method used in the software is based on the assumption that the vehicle pass-by noise is a superposition of several principal noise sources. The characteristics of each sound source are defined as physical models by using the measurements which were made at operating conditions. The positions of the sound sources are determined and are given into the software as an input. In the methodology, Doppler Shift is corrected (Dopplerization) in the frequency and amplitude parts of the measured signal and reflection of sound wave on ground (asphalt road surface) is counted. Finally, by summing up all of the contributions due to each principal sound source, an overall pass-by noise data is provided.

Airborne Source Quantification (ASQ) is a technique that is utilized by Fleszar, Linden, Johnsen and Grimmer for prediction of pass-by noise level of a vehicle which is based on the measurements made indoors [15]. In this technique, propagation characteristics of the noise emitted from different sources on the vehicle is described as the acoustical transfer functions between the source and the receiver (which is the microphone positions with respect to vehicle as in the case of standard pass-by noise test). To apply this technique, the transfer path between the source and the receiver should be airborne as in the pass-by noise tests. Acoustical source strength of each principal sound source on the vehicle is proposed to be measured in two ways using experimental techniques. One of them is direct measurement; the other is indirect calculation by using the transfer matrix inversion method. Also, acoustical transfer functions between the receiver and source are proposed to be obtained from either indoor or outdoor measurements. Then, superposition of all individual source contributions is calculated and an overall pass-by noise level with respect to vehicle position can be achieved by using this technique.

Another study was performed by Fujita, Abe and Hori in 1980s which aimed to develop a technique based on the fact that vehicle noise consists

of four principal noise sources which are engine, exhaust discharge, exhaust surface and tire [22]. Propagation model for engine noise is achieved using empirical information such that sound power level of the engine is calculated by using the measurements underneath the oil pan. To be able to obtain the angular radiation information of the noise, several measurements were made and sound directivity indexes are calculated. In this study, engine noise radiation characteristics of two different engine layouts (longitudinal and transverse mounted) were investigated to improve the accuracy of the simulation. In the case of propagation model for exhaust discharge, ground reflection effects were also considered. Tire noise is modeled as a point source. Acceleration profile of the vehicle is achieved by using equation of motion for the vehicle with several parameters (vehicle weight, gear ratios, engine output torques). Finally, combining all information above, an overall pass-by noise level of the vehicle is calculated with respect to its position.

Park and Kim investigated two different methods for prediction of pass-by noise in a semi-anechoic chamber in their study [23]. First one is based on the measurements using line array microphones and spherical Hankel functions to represent the spherical harmonics of free space sound field. It is stated in the paper that if the measurements are not made in the near field where spherical Hankel coefficients can distinguish from each other, this method gives serious errors. In the second method, Nearfield Acoustic Holography (NAH) was adopted for prediction of pass-by noise. Measuring acoustic pressure on the hologram plane with respect to RPM of the vehicle in the range of the acceleration profile is stated to be the major drawback of implementation of NAH. Wrap-around errors, aliasing and errors due to finite aperture size are cited. In the study, analysis and measurements at one specific RPM were made for comparison with the results acquired from outdoor pass-by noise measurement. In their second study, an improved method called "Moving Frame Acoustic Holography" is developed. The

method is proposed to overcome errors due the finite aperture size [24, 25]. In the new method, the aperture size of the hologram and spatial resolution are noted to be increased.

2.5 Beamforming and Nearfield Acoustic Holography

In general, there are two main techniques in measuring the noise and mapping the sound intensity in the case of a moving sound source. One of the techniques is based on beamforming algorithm. In beamforming, several non-directional microphones record the signals and then delay term is introduced to each corresponding signal with respect to the microphones positions, directions and frequency. However this algorithm is based on the fact that sound waves are plane waves, not spherical waves. So it is applied to the far-field. The other technique which is widely used is based on Nearfield Acoustic Holography (NAH) algorithm. In this technique, there is a measurement plane called hologram plane which consists of number of microphones. The recording of the sound pressure in this plane are then used to construct the sound intensity map. Acoustic field at any distance from the hologram plane can be calculated.

2.5.1 Beamforming

Beamforming technique is quick way of mapping sound intensity levels. Since noise source identification is becoming more and more important, especially to car manufacturers, this technique along with other alternative techniques is often utilized. Also, researchers keep still working on this technique to improve it [26-30].

Beamforming technique is based on the measurements at a number of microphone positions at some distance from the object. When the microphones are placed in the far field, the sound waves hitting the array are approximated by plane waves (Figure 2.7).

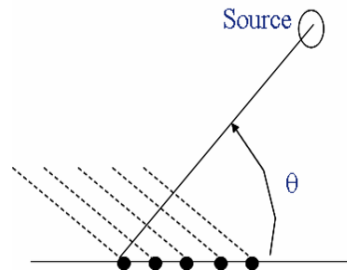


Figure 2.7 Plane waves hitting the microphones in the far field [30]

When the source is moving, then the sound at a point in the distance will be perceived like it changes in time. This is due to the Doppler Effect. To overcome this problem, “De-dopplerization” operation is to be applied. This is done by introducing specific delays on each microphone with respect to their positions and the directions between the sound sources (Equation 2.1). Delays are also related with the frequency itself. So, that makes this technique more challenging to implement. In the application of this technique, 2-D or even 3-D dimensional microphone arrays are used. A. Cerniglia and M. Lenti explained this technique briefly and gave good examples of application of this technique on different problems [26].

There is some literature on the analysis of utilizing beamforming technique to predict pass-by noise. H. Kook, G. B. Moebis, P. Davies and J. Bolton explained briefly about beamforming technique in their paper [31]. Stationary array of microphones were used to visualize the noise sources of a vehicle while it is accelerated in outdoor. Although several approaches on Doppler shift, time delay and spherical spreading corrections were used in their study, this technique should be investigated and checked for adoption

to indoors. Also, S. Parker and Y. Kim compared beamforming with NAH results in their paper [23]. However, this technique was not found to be applicable for prediction of vehicle pass-by noise phenomena. Several researchers have papers about locating sound sources of road vehicles using beamforming [32-34]. The methods they used are all applicable in outdoor measurements. Thus, new approaches are needed to adopt their studies into vehicle pass-by noise indoor measurements.

2.5.2 Nearfield Acoustic Holography (NAH)

Near Field Acoustical Holography (NAH) technique was developed in the eighties by Maynard, Williams, Lee and Veronesi. It has been widely recognized as a useful tool to localize and quantify sound sources [35-37]. In this technique, there are mainly three steps; measurement of the sound pressure on the hologram plane, prediction of acoustic variables on desired plane whether closer to the source or further from the source, and reconstruction of the sound intensity map.

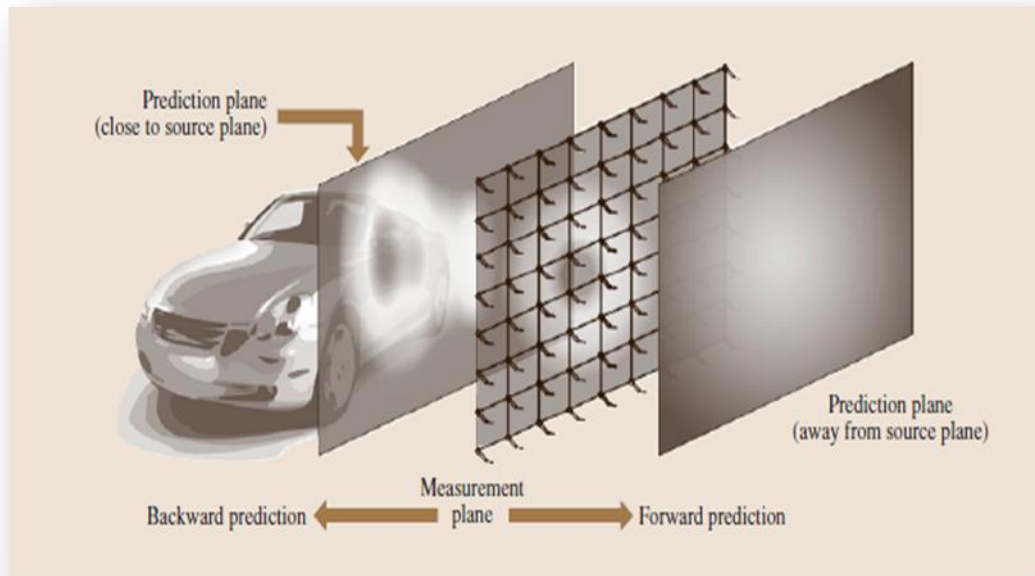


Figure 2.8 Illustration of Acoustic Holography [12]

In the measurement step, sound pressure is measured at specific points by microphones on measurement plane called "hologram plane". While doing this measurement, care should be taken such that aliasing, wrap-around errors do not occur. P.R. Stepanishen, K.C. Benjamin gave such details in their paper [38]. Also E.G. Williams and J.D. Maynard briefly explained in their papers about this procedure and its methodology [35-37]. Many researchers and engineers have worked on Nearfield Acoustic Holography and some of them have tried to extend this algorithm on different applications while others have tried to fix the drawbacks of the NAH method and make it better [39-44].

While predicting the sound level of a pass-by vehicle according to ISO 362, NAH was utilized by S.H. Parker and Y.H. Kim. They explained their analysis and tests in their papers [23]. They also went one step further and used moving frame acoustic holography [24, 25]. To form a hologram plane, they used a line array of microphones which is swept along a stationary

sound field. In their research, they assumed that the pass-by noise of a vehicle is quasistationary and frequency change of the noise is also negligible. With these assumptions, the scanning plane is extended which allows measuring the moving sound sources like vehicle's exterior noise and spatial resolution of the hologram is increased. In the next step, they tried to overcome one major drawback of this method that it can be applied only to sinusoidal components. They improved the method so that it can also be applied to band limited and transient noise.

Spherical microphone arrays have attracted attention increasingly especially for source identification because of their advantages in specific applications. F. Jacobsen, G. Moreno, E. Grande and J. Hald investigated the method of using rigid sphere in spherical near field acoustic holography[45]. Rigid sphere is considered to have more advantages than open sphere like the boundary conditions can be better defined by using rigid sphere. Indeed, rigid spheres are used with beamforming method in which measurement point is in the far field. When using rigid sphere in NAH which is a near field technique, there exists a problem. Since the measurements are taken fairly close to the sound source, sound waves diffused from the rigid sphere will probably be reflected by the surface of the sound source. In their research, they investigated the case by a simulation study and experimentally. As a result, they have found out that it does not create serious errors.

NAH has some limitations and errors due to the assumptions made at the beginning of the method. One of them is mainly consists of errors in the reconstructed acoustic image. A. Fernandez, E. Silla, R. Soriano and R. Tormos worked on this problem and extended a new technique called "Selective Near Field Acoustic Holography" which improves the resolution of the image [46]. In NAH filtering is applied to eliminate the effect of errors due to the phase of the signals which is resulted from the different positions of the microphones. However while filtering; the resolution of the image is

reduced. In this technique, they have tried to fix this problem by making an extra measurement with an accelerometer and getting a coherence function between the signals from the hologram and the accelerometer. This procedure reduces the measurement error and the resolution is improved.

In analyzing the cyclostationary sound field, traditional NAH technique is not sufficient. Q. Wang and W. Jiang proposed a new technique called Cyclostationary NAH (CYNAH) to reduce the limitations and errors of NAH [47]. In this new technique, sound pressure is displayed by cyclic spectral density (CSD) instead of power spectral density (PSD). However, CYNAH proposed is only applicable if there is a single sound source or multiple dependent sources. This technique is extended apply to multiple independent sound sources. It is proposed scan based measurement to construct a complete hologram by joining together sub holograms captured using a moving scan array and a fixed multi reference array. And a procedure was applied to remove the influence of sampling time delay, finite data length and source level variations in constructing the complete hologram.

Sound sources should be fully coherent to apply traditional NAH. However, in many problems this is not the case. Sound fields consist of many incoherent sound sources. To eliminate this limitation, D. Hallman and J. Bolton proposed an extended technique called Multi-Reference NAH [48]. In this technique multi reference microphones are used instead of a single one. Transfer functions between the reference signals and the corresponding parts of the hologram are derived to get the phase relations associated with the incoherent sources. However, the number of reference signals should be sufficient so that the prediction of the sound pressure is within the experimental error. Since it is not possible to have the number of the reference microphones as many as incoherent sound sources, this proposed technique is not applicable.

In some applications, relatively low sound leveled sources are to be measured. To get a high resolution of sound field, poor signal to noise ratio should be eliminated. B. Roozen, W. Potze and E. Mulkens extended the traditional NAH using cross-spectral density functions and tried to get a higher signal to noise ratio [49]. Thereby, it enables a higher resolution of the reconstructed sound field. The limitation of this technique is that it can only be applied to stationary sound sources since measurement of cross spectral densities is done with time averaging.

NAH has great advantages. On the other hand, there are limitations when applying this technique to analyze the sounds with high frequencies. F. Deblauwe, K. Janssens and B. Beguet proposed a beamforming based technique that can extend the frequency range to higher frequencies and can also increase the frequency range while the spacing between the microphones are kept the same [29,30]. Indeed, focalization is beamforming technique which is applied in the near field as in the case of NAH. It uses the fact that the sound waves hitting the line array is not planar waves but spherical waves. A phase correction in the function of radius of the wave is applied to the basic equation of the beamforming (Equation 2.1). This technique also extends the usability of beamforming.

Direct use of NAH puts some limitations on the application. Spatial Transformation of Sound Fields technique was proposed by J. Hald to overcome the restrictions such that NAH was only applicable to coherent sound sources [50-52]. Instead of using the power spectral density, in this technique, cross spectra between reference microphones and hologram grid positions are taken. Then from the measured cross spectra, holograms are calculated that can be applied in connection with NAH. The main advantage of this technique is that it can be applied to non-coherent sound sources without the need for simultaneous measurements. As in the other NAH measurement techniques sound source must be stationary. That is one of

the drawbacks of the technique along with the fact that it needs large number of measurements when the sound source is a large and complicated broad-band source.

CHAPTER 3

THEORETICAL CONSIDERATIONS AND DEVELOPMENT OF THE PROPOSED METHOD

3.1 Time Records and Frequency Spectrum

Signal processing plays an important role in acoustical engineering such that it covers acquisition, storage, display and generation of signals. Generally signal data is classified as in Figure 3.1 [53].

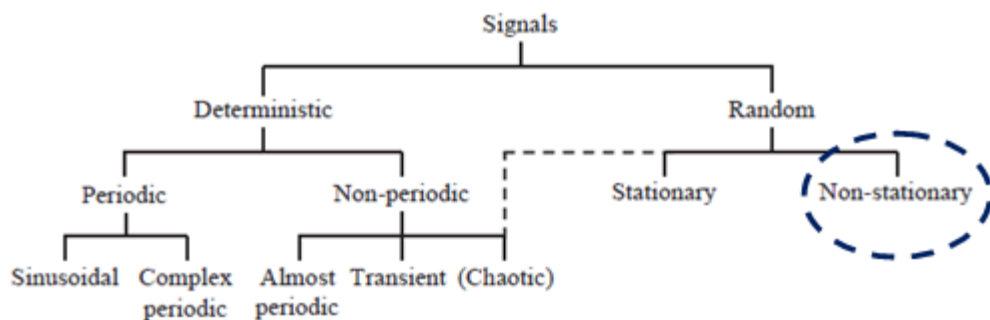


Figure 3.1 Classification of Signals [53]

In many branches, random signals and noise which do not have a precise mathematical description are often encountered. Common example to random signals is vehicle noise on a road. While the characteristic of

random signal is dependent on time, it can be classified into two subgroups. If the statistical properties do not change under a shift in time, it is called stationary; else it is called non-stationary [54]. The pass-by noise of vehicle can be regarded as non-stationary random signal if it is classified according to Figure 3.1.

3.2 Plane and Spherical Waves

Linearized, unforced wave equation expressed in terms of acoustic pressure is given by,

$$\nabla^2 p = \frac{1}{c^2} \frac{\partial^2 p}{\partial t^2} \quad (3.1)$$

The solution to this equation is generally obtained for either one-dimensional or three dimensional sound waves.

3.2.1 Plane Waves:

For plane wave propagation, assuming that sound pressure varies in only one dimension, linearized wave equation i.e. x direction reduces to;

$$\frac{\partial^2 p}{\partial x^2} = \frac{1}{c^2} \frac{\partial^2 p}{\partial t^2} \quad (3.2)$$

By introducing a new variable "u=x-ct", the general standing wave solution to Equation (3.2) is obtained as;

$$p(x,t) = f(x - ct) + g(x + ct) \quad (3.3)$$

Properties of Plane Waves are simply stated as;

- Progressive plane waves radiate in one direction,
- Sound pressure amplitude is constant over distance,
- The sound intensity "I" is proportional to P_{rms}^2 ,
- Acoustic pressure, particle velocity and density changes are in phase for positive traveling plane waves.

3.2.2 Spherical Waves:

If the solution for the unforced linearized wave equation is obtained in spherical coordinates, then Equation (3.1) becomes;

$$\frac{\partial^2(rp)}{\partial r^2} = \frac{1}{c^2} \frac{\partial^2(rp)}{\partial t^2} \quad (3.4)$$

And the general solution to Equation (3.4) is;

$$p(r,t) = \frac{1}{r} f(r - ct) + \frac{1}{r} g(r + ct) \quad (3.5)$$

Since the second term (incoming wave) in Equation (3.5) does not satisfy Sommerfeld radiation condition, only the first term (outgoing wave) is taken into account. Another representation of outgoing wave which will be used later in this chapter is;

$$p(r, t) = \frac{A}{r} e^{j(\omega t - kr)} \quad (3.6)$$

For larger values of r (with respect to the wavelength, $\lambda (= c / f)$), first term in Equation (3.7) can be neglected, and the solution looks like a plane wave solution. Properties of spherical waves can be considered in the case of near field or far field situations;

In the far field;

- Sound pressure amplitude is inversely proportional to the distance " r ",
- Sound intensity " I " is proportional to " A^2 / r^2 ",
- Pressure and velocity gradients are in phase.

In the near field;

- Complex valued relationships between " P , u and r " exist.
- Acoustic pressure and particle velocity in radial direction have phases of almost 90° depending on the value of kr .

3.3 Sound Fields in Enclosed Space

The easiest way to investigate an acoustical problem is to consider the sound in a field where it is not reflected, undiffused and undiffracted. This theoretical field is called "free field". Owing to the property of absence of reflective surfaces, the conditions of free field are almost satisfied in

anechoic rooms. For a better understanding and solving an acoustical problem, four types of sound fields are defined around a noise source.

Near Field: Near field is the area very close to the sound source where there is significant change in the sound pressure with respect to the position. Practically; the border of this field is taken as the wavelength of the lowest frequency emitted or twice the greatest dimension of the source (whichever is the greater).

Far Field: The area which is further from the sound source and exists after near field is called "far field". In this region, sound sources are generally regarded as "point sources". It consists of "free field" and "reverberant field" (and a transition region between them).

Free Field: In this region, sound travels without any interference. If the sound source is a point source, then doubling the distance from the source will result in a 6 dB drop in the sound pressure level. (Figure 3.2)

Reverberant Field: In the reverberant field, level of the reflected sound wave from walls or any reflective objects is almost as high as direct sound level. That will cause the sound pressure level remains constant while the distance from the sound source increases. Such a field is termed as diffuse field (Figure 3.2).

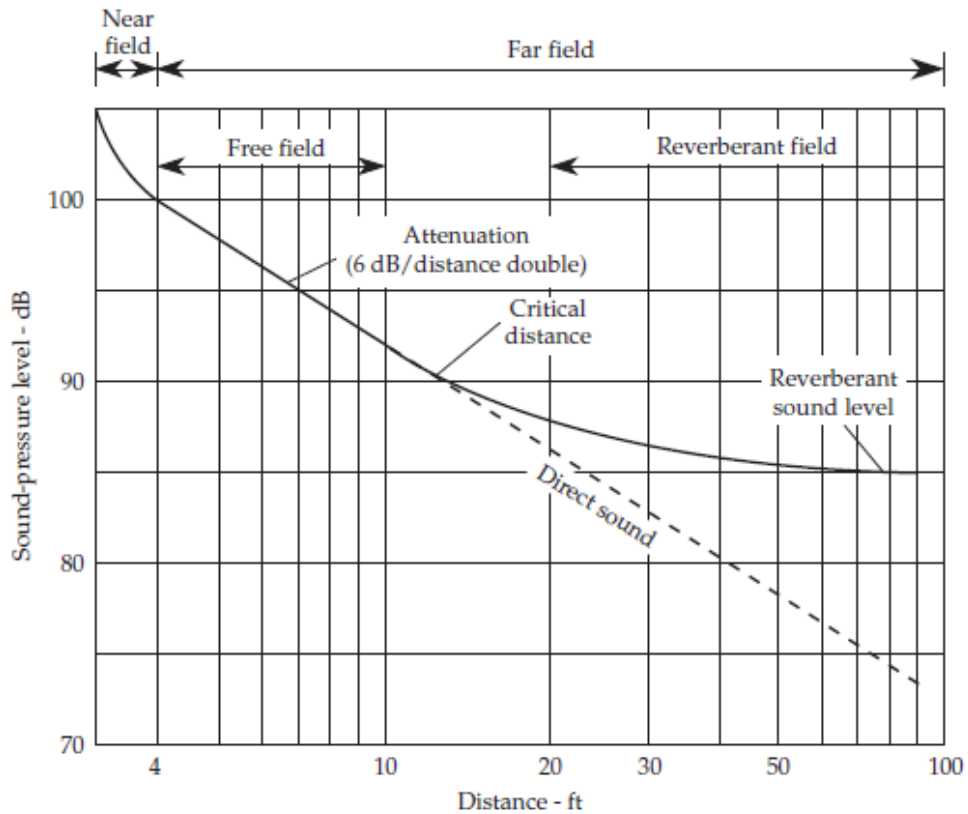


Figure 3.2 Sound Fields in Enclosed Spaces [11]

3.4 Type of Sound Sources

There are almost an infinite number of different types of sound sources regarding their geometries and radiation of noise is generally a complicated problem. However, in engineering noise control applications, some simple sound source models regarding their geometries are used for reproduction of sound and analysis of the problems. In the scope of this study, two types of them will be investigated.

3.4.1 Point Sources

The point source (monopole) is a compact sound source which emits sound equally in all directions. The simplest example of a point source is a pulsating sphere whose radius enlarges and decreases sinusoidally. (Figure 3.3)

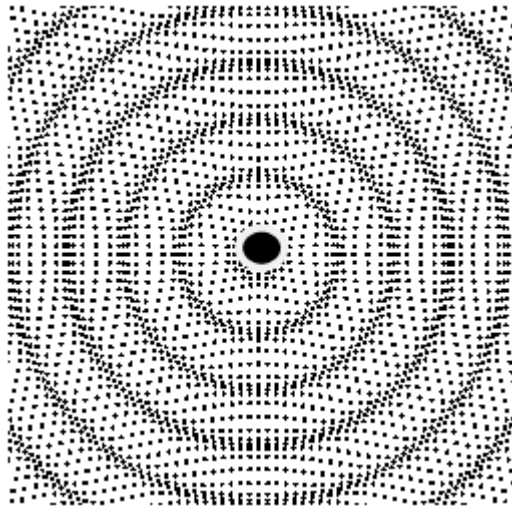


Figure 3.3 Illustration of Monopole Source

Through this action, the sphere introduces and removes certain amount of volume of the medium into the surrounding area. It is denoted by "Q" and called volume velocity, expressed in m³/s. Sound pressure produced by a point source at distance r in free field is equivalent to;

$$P(r, t) = \frac{j\omega\rho_0\tilde{Q}}{4\pi r} e^{j(\omega t - kr)} \quad (3.7)$$

Here, $k=\omega/c$ is the wave number and \hat{Q} indicates that it has a complex value. From Equation (3.7), it can be clearly seen that sound pressure is inversely proportional to the distance (r). It means that doubling the distance from the sound source will result in a 6 dB decrease in sound pressure level in free field conditions. Sound intensity of a point source is;

$$I(r) = \frac{\rho_o \hat{Q}^2 \omega^2}{32c\pi^2 r^2} \quad (3.8)$$

And from this equation, it can be understood that sound intensity "I" is inversely proportional to the square of the distance.

3.4.2 Line Sources

Line sources are combination of point sources which are linearly positioned (Figure 3.4). Each of the sound sources is assumed to be equally distanced "d" from each other with the same sound power (W_o).

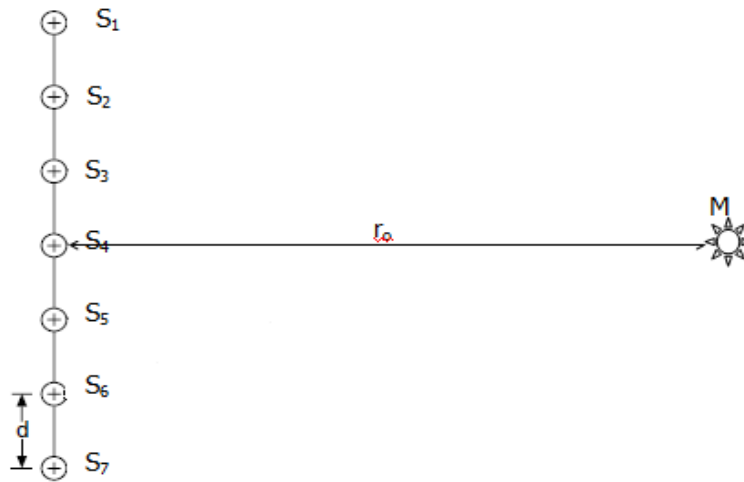


Figure 3.4 Illustration of Line Source

Sound pressure level can be found in the case of two different cases [7]. If the sound sources are incoherent;

$$L_p = L_w - 6 - 10 \log_{10}(r_o) \text{ (dB)} \quad (3.9)$$

And if the sound sources are coherent;

$$L_p = L_w - 8 - 10 \log_{10}(r_o) \text{ (dB)} \quad (3.10)$$

According to Equation (3.10) and (3.11), rate in the divergence of the sound pressure level is -3 dB per doubling the distance from the sound sources. It should be noted that, these implications are true if the distance (r_o) is not greater with respect to the length of the array of sources. A common example of this type of source is road traffic noise.

3.5 Sound Emission from Moving Sources and Doppler Effect

During a vehicle pass-by noise outdoor measurement, due to the relative motion between the fixed microphones and the moving vehicle, a phenomenon called "Doppler Effect" occurs. Since it leads to amplitude and frequency change in the received signal, it is necessary to consider its effect on the measurements done in semi-anechoic room for pass-by noise prediction.

For a better understanding the problem, a point source moving only in one direction (x – direction) is considered [33].

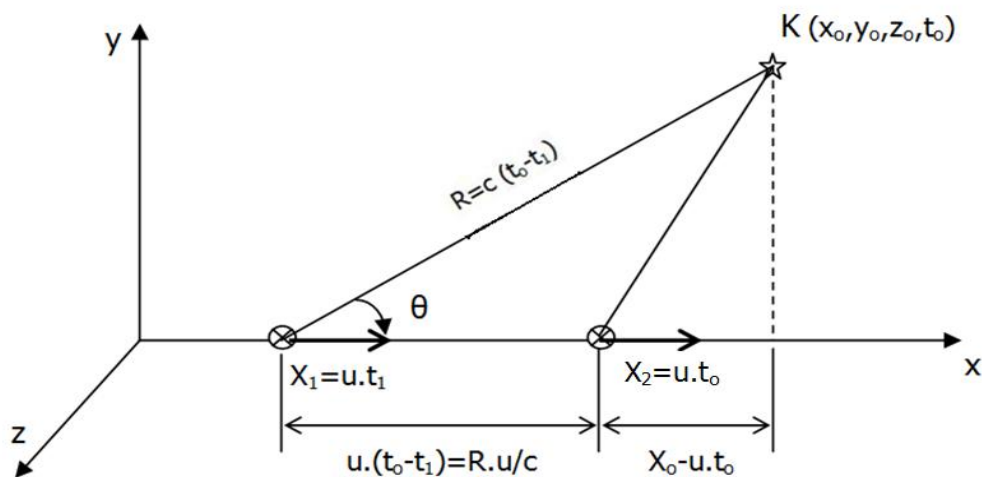


Figure 3.5 Kinematics of a Moving Point Source

The receiver point is fixed at K with coordinates x_o , y_o and z_o . The sound radiated from the moving source at the time $t=t_1$ reaches point K at the time $t=t_o$. So, the time delay is $T=t_o-t_1$. The distance denoted by R can analytically be found as;

$$R^2 = \left[x_o - u \left(t_o - \frac{R}{c} \right) \right]^2 + y_o^2 + z_o^2 \quad (3.11)$$

Here, “ u_{vech} ” is the velocity of the moving source in x-direction. By introducing the Mach Number “ $M=u_{\text{vech}}/c$ ” and $r_o^2 = y_o^2 + z_o^2$, Equation (3.11) takes the form;

$$R = \frac{M(x_o - u_{\text{vech}} \cdot t_o) \pm \sqrt{(x_o - u_{\text{vech}} \cdot t_o)^2 + (1 - M^2)r_o^2}}{1 - M^2} \quad (3.12)$$

It should be noted that in pass-by noise measurements, the speed of the vehicle “ u_{vech} ” is smaller than the speed of the sound “ c ”. In this case ($M=u_{\text{vech}}/c < 1$, subsonic motion), only the positive sign in Equation (3.12) gives a positive value for “ R ”.

To make the analysis easier to be understood, R_1 is introduced such that [33];

$$R_1 = \sqrt{(x_o - u_{\text{vech}} \cdot t_o)^2 + (1 - M^2)r_o^2} \quad (3.13)$$

Equation (3.12) is then reduced to;

$$R = \frac{M(x_o - u_{\text{vech}} \cdot t_o) \pm R_1}{1 - M^2} \quad (3.14)$$

By using the angle "θ" between the direction of motion of the moving source and the direction of the position vector "R", R_1 can also be written as;

$$R_1 = R * (1 - M \cos \theta) \quad (3.15)$$

In the next stage of the analysis, sound pressure field of the moving source will be investigated. As already indicated, the point source was considered. The source distribution of the point source, moving only in the x-direction is;

$$\Phi = Q \cdot \delta(x - u_{veh} \cdot t) \cdot \delta(y) \cdot \delta(z) \quad (3.16)$$

Here, Q is the acoustical source strength. If this is implemented into the wave equation, it becomes;

$$\nabla^2 P - \frac{1}{c^2} \frac{\partial^2 P}{\partial t^2} = - \frac{\partial}{\partial t} Q_{(t)} \cdot \delta(x - u_{veh} \cdot t) \cdot \delta(y) \cdot \delta(z) \quad (3.17)$$

And by introducing;

$$P = \frac{\partial \Psi}{\partial t} \quad (3.18)$$

The equation (3.17) can be written as;

$$\nabla^2 \Psi - \frac{1}{c^2} \frac{\partial^2 \Psi}{\partial t^2} = -Q_{(t)} \cdot \delta(x - u_{vesch} \cdot t) \cdot \delta(y) \cdot \delta(z) \quad (3.19)$$

One of the ways for solving this equation is using a linear transformation based on Lorentz transformation [33]. After transforming the coordinates, the solution can be obtained as;

$$\Psi(\bar{r}, \bar{t}) = \gamma^2 \frac{Q\left(\bar{t} \pm \frac{\bar{r}}{c}\right)}{4\pi\bar{r}} \quad (3.20)$$

Here;

$$\bar{t} = \gamma \cdot t = \gamma^2 \left(t - \frac{u_{vesch} \cdot x}{c^2} \right),$$

$$\bar{x} = \gamma \cdot x = \gamma^2 (x - vt),$$

$$\bar{y} = \gamma \cdot y = \gamma \cdot y,$$

$$\bar{z} = \gamma \cdot z = \gamma \cdot z ,$$

$$\bar{r} = \sqrt{\bar{x}^2 + \bar{y}^2 + \bar{z}^2} , \quad (3.21)$$

where, $\gamma = \frac{1}{\sqrt{1-M^2}}$ and $M = u_{\text{vech}}/c$.

In the case of the subsonic motion, only the plus sign in Equation (3.20) can be used. If transformation back to the initial coordinates is applied;

$$\Psi(r, t) = \frac{Q\left(t - \frac{R}{c}\right)}{4\pi R_1} \quad (3.22)$$

And the sound pressure field is then;

$$P = \frac{\left(1 - \frac{1}{c} \frac{dR}{dt}\right) \dot{Q}\left(t - \frac{R}{c}\right)}{4\pi R_1} - \frac{Q\left(t - R/c\right) dR_1}{4\pi R_1^2 dt} \quad (3.23)$$

By using the formulation between R and R₁ (Equation 3.15), the final form of the equation turns out to be as;

$$P = \frac{\dot{Q}\left(t - \frac{R}{c}\right)}{4\pi R(1 - M\cos\theta)^2} + \frac{Q(\cos\theta - M) \cdot u_{veh}}{4\pi R^2(1 - M\cos\theta)^2} \quad (3.24)$$

The first term in Equation (3.24) simply indicates the pressure change with respect to the distance R and also shows that Doppler Effect on the amplitude of the signal which is emitted at time $t=t_1$ is;

$$A_{Dop}(t_1) = \frac{1}{(1 - M\cos\theta)^2} \quad (3.25)$$

The interpretation of this result is that sound pressure is amplified when the source is coming towards the receiver ($0 < \theta < 90$), and it is decreased when the source is going away from the receiver ($90 < \theta < 180$).

Another change happens in the frequency domain of the emitted signal.

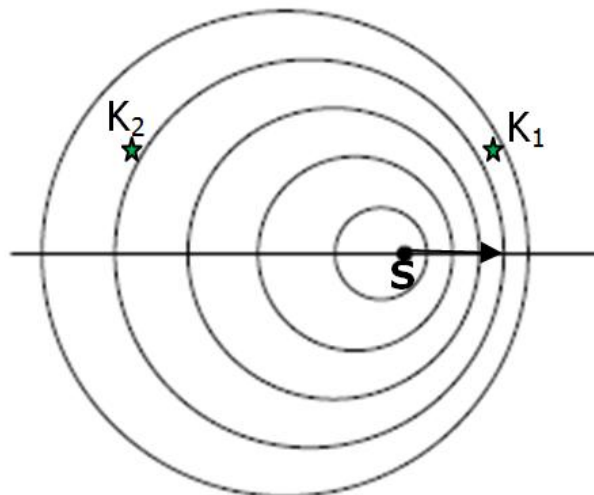


Figure 3.6 Moving Point Source (Subsonic Motion)

As it can be seen from Figure 3.6, the wave fronts are not concentric in the case of the moving source. If the receiver position is in front of the sound source, due to the decrease in the wavelength, the frequency at point K_1 perceived higher than the original frequency ($0 < \theta < 90$).

$$f_{K1} = \frac{f_o}{1 - M \cos \theta} \quad (3.26)$$

If the receiver position is behind the source, due to the increase in the wavelength, the frequency at the point K_2 perceived lower than the original frequency ($90 < \theta < 180$).

3.6 Experimental Studies On Indoor Vehicle Pass-by Noise Measurements

In accordance with the technological developments in both room acoustics and data acquisition systems, it is becoming very important to predict vehicle pass-by noise level during vehicle development steps. Thus, it is rather more practical to measure vehicle pass-by noise in a semi-anechoic acoustic room, as well as it provides significant time savings. However; to be able to perform a pass-by test indoors, equivalent conditions with the outdoor measurement described in ISO 362 must be satisfied.

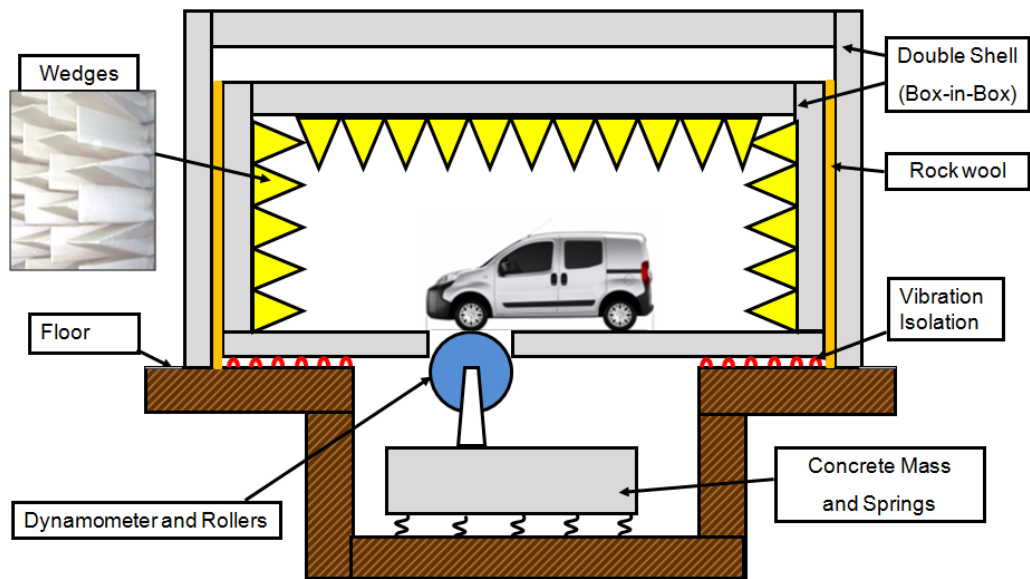


Figure 3.7 Illustration of Measurements in a Semi-anechoic Room

3.6.1 Room and Dynamometer Requirements

The fundamental requirement stated in ISO 362 is that the test area must be free from any acoustically reflective objects at least in a radius of $r=50\text{m}$. In other words, it must be free field with reflective ground. This condition can be established in a semi-anechoic room which has good reverberation characteristics and has a low cut-off frequency. The sound wave absorption mechanism inside the room is illustrated in Figure 3.8.

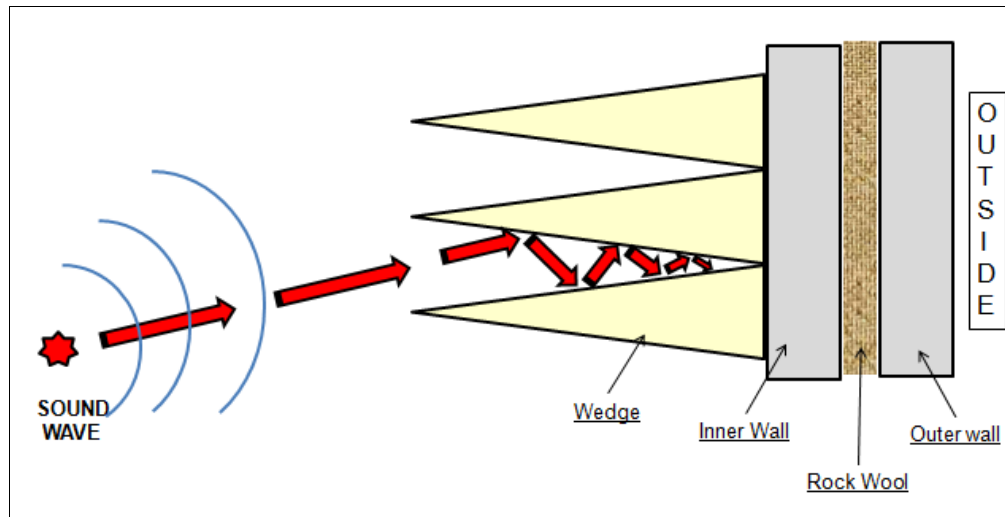


Figure 3.8 Sound Absorption Mechanism inside the Acoustic Room

Glass wool wedge modules which have high absorption coefficient are used on the surfaces of the walls. As a rule of thumb, microphones can be positioned at least quarter wavelength of the lowest frequency of interest. The cut-off frequency of the room is dependent on the length of wedges. Since there is no noticeable frequency component under 100 Hz in pass-by noise spectra of road vehicles, the cut off frequency of $f_c=50$ Hz will be a rather trusted value.

Another requirement is that the room must satisfy the inner dimensions which are shown in Figure 3.9. The lateral dimension (inner) of the room must be at least 15 m plus 2 m; so that microphones can be positioned 7.5 m from the centerline of the vehicle and reflections due to the walls (which are assumed to have little effect) are avoided. Also; assuming the vehicle has a typical length of around 5 m, the length of the inner dimension of the room must be at least 20 m i.e., the length of the test track, plus the length of the vehicle (5 m) and microphone spacing from the walls (1+1=2) which makes up 27 m.

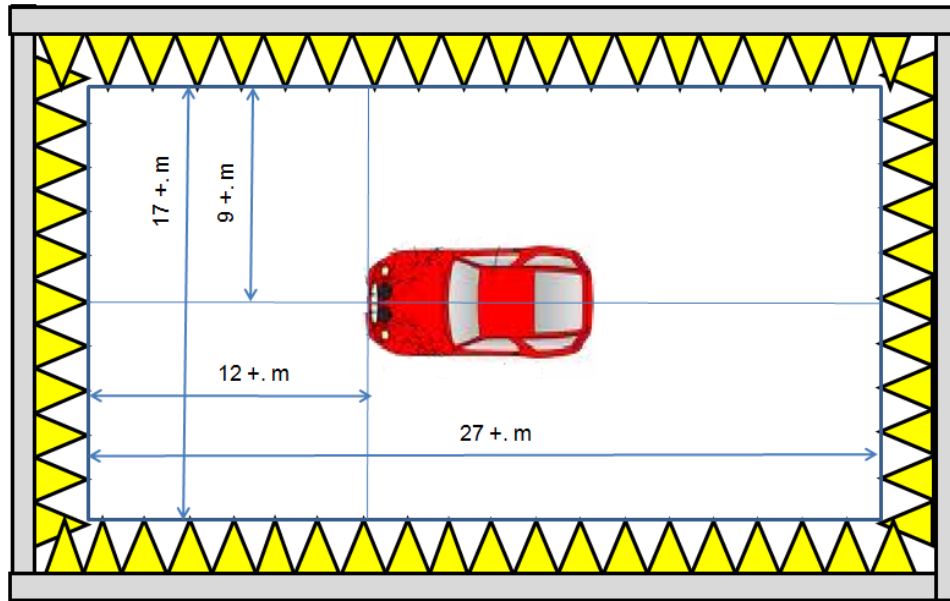


Figure 3.9 Limiting Values for inner Dimensions

The dynamometer must have an equivalent response with the vehicle acceleration conditions as in the outdoor measurements. Also; while testing, the sound pressure level due to the dynamometer operation must be at least 15 dBA below the recorded sound level of the vehicle. According to the fact that lowest sound pressure level recorded at third gear which is typically around 70 dBA, sound pressure level of 50 dBA for background noise due to the dynamometer operation is regarded to satisfy the background noise requirement for such measurements. The roller surface which interacts with the tire must have equivalent characteristics with the asphalt road surface complying with ISO 10844 [1].

3.6.2 Microphone Placement and Data Processing

While the vehicle is accelerated as in the outdoor tests, sound pressure signals can be recorded in two ways; either with moving microphones which translates relative to the stationary vehicle or with an array of microphones

placed aside parallel to the vehicle. The greater number of microphones is used in the test, the more detailed and accurate measurements can be made. Time signals from each microphone are used successively in accordance with the vehicle position which can be acquired by taking the integral of the speed data of the vehicle.

3.6.3 Comparison of Indoor and Outdoor Pass-by Noise Measurement

Although some conditions mentioned above can be satisfied in indoor measurements, there will be still some differences. One of them is the rear tire noise (or front tire noise) which is not operated from the dynamometer, will be absent. Likewise, wind noise which is regarded to have very little effect on the overall pass-by noise for the vehicle test speed range will be absent either.

Another difference is that vehicle is moving with respect to the microphone position which produces frequency and amplitude shift in the recorded signal in the case of outdoor test. On the other hand; there is no such thing in indoor measurement unless the microphone is moving with respect to the vehicle. Dopplerization procedure which transforms the signal and add shifts into both frequency and amplitude can be applied to fix this situation and match the conditions in the outdoor tests.

Also; the tire-asphalt road surface interaction will surely be different from the tire-roller surface interaction. Thus, the noise characteristics will not be the same. Another important point is that sound wave reflection and diffraction characteristics on asphalt surface will not be identical to the one on the acoustic room floor surface which is made up of concrete and covered with special treatment.

Table 3.1 Comparison of Outdoor and Indoor Pass-by Noise Measurements

Outdoor Pass-by Noise Measurement (ISO 362)	Indoor Pass-by Noise Measurement
Semi-anechoic free field	Semi-anechoic free field
Moving vehicle (Inherit Doppler shift)	Stationary vehicle
The test site has a length of 20m + length of the vehicle (4m – 6m for passenger cars) and has a width of 15 m	It should be at least 27m in length and 17m in width
All tires are operating	Only front or rear tires are operating
Tire-asphalt Interaction	Tire-Roller Surface Interaction
Aerodynamic Noise	No Aerodynamic Noise
Earth and Asphalt Surface Reflection	Acoustic Room Floor Surface Reflection

3.7 General Overview of the Semi-anechoic Room

The general aim of this study is stated as to come up with a new method for indoor pass-by noise measurements. The method will be applied to such measurements taken in semi-anechoic room belonging to R&D Department of TOFAS. Thus, the acoustical performance of the room must be investigated along with its general specifications.

The structure of the semi-anechoic room is like a box within a box as shown in Figure 3.7. The inner dimensions (from/to tip of the wedges) of the room are 17.4 x 12.1 x 4 in meters. The position of the rollers is centered as in Figure 3.10. As it can be seen from the figure, the rollers are not centered laterally in the room. The distance from the centerline of the rollers to the right side of the room (to the tip of the wedges) is 7.5 m; however, to the left side of the room is 4.7 m. This means that the room lacks sufficient width and length for measuring the pass-by noise as mentioned earlier in Section 3.6.1. Also, one has to consider that the distance from the car centerline to the each side is not same. In other words, if the pass-by noise levels for both right and left sides of the vehicle are desired to be measured simultaneously, then one has to develop a method appropriate to the shortest distance which is 4.6 m.

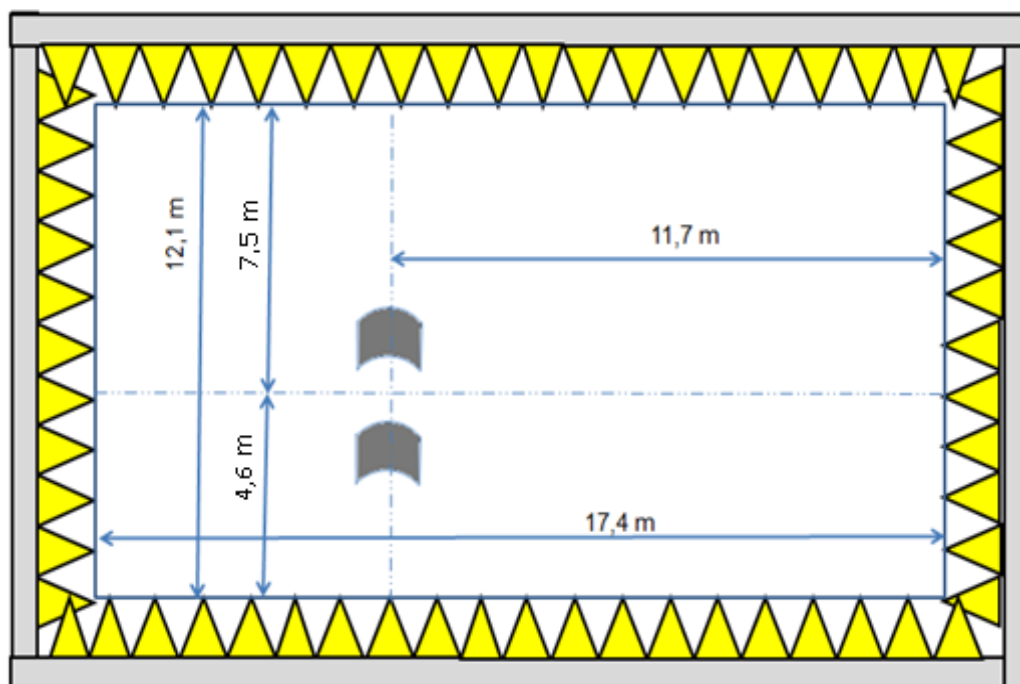


Figure 3.10 Position of the rollers in the room

3.7.1 Acoustical Specifications of the Room

In order to evaluate data acquired from the measurements of sound pressure in a semi-anechoic room, the quantitative effects of sound reflection and scattering within the room must be known. Generally, three acoustical parameters are considered when investigating such rooms.

The first one is the cut-off frequency which gives information about the frequency range over which acquired data is regarded to be reliable. There are several methods to specify the cut-off frequency of the room. The most common one is making measurements of sound pressure while an omnidirectional sound source is fixed and the measuring microphone is moved apart. Deviations of the sound pressure levels from the inverse square law are determined from the measurements to evaluate the extent of discrepancies from free field conditions.

Other acoustical parameter is reverberation time. Reverberation time is affected by the size of the space and the amount of reflective or absorptive surfaces within the space. A room with highly absorptive surfaces will absorb the sound and prevent it from reflecting back into the space. This would yield a space with a short reverberation time. Reflective surfaces will reflect sound and will increase the reverberation time within a room. In a semi-anechoic room the requirement is to have short reverberation times.

The last parameter is the background noise level. It is level of the sound pressure when there are no operating sound sources in the environment. In addition, the noise level while the chassis dynamometer is operating must also be checked. While simulating pass-by noise in the room, this level must be under 55 dBA at the rolling speed of 60 km/h.

The acoustical parameters of the semi-anechoic room in NVH Department within R&D Center of TOFAS are given in Table 3.2. The cut-off frequency of 50 Hz is suitable for pass-by noise testing since the frequency

range of interest is between 50-8000 Hz. The background noise levels without and with the dynamometer operating are quite low. Reverberation time performance of the room can be regarded to be good, since the target value for such semi-anechoic rooms is 0.1 second. Consequently, the acoustical capability of the room can be regarded to be high for indoor pass-by noise measurement purposes.

Table 3.2 Acoustical performance of the semi-anechoic room in TOFAŞ

Acoustical Parameters	Values
Cut-off Frequency	50 Hz
Reverberation Time between 100 Hz and 5000 Hz	0.14 second
Background Noise Level	17 dBA
Noise Level When the Dynamometer Speed is 100km/h	48 dBA

3.8 Noise Source Investigation of the Vehicle

The acoustical model of the vehicle must be developed before starting the pass-by noise prediction process. The exterior noise characteristics of automobiles were already discussed in Section 2.2. Based on this information and prior experimental experiences, it was decided to handle the noise sources of the vehicle in three sub groups regarding their locations on the vehicle. These are;

- 1- Engine Noise including air intake and transmission noise,

- 2- Tire-Road Noise,
- 3- Exhaust Orifice Noise.

The contribution of each group was investigated in several experimental cases and the preliminary tests were performed on a specific vehicle to justify the proposed method. The following sections are dedicated to the experimental investigation of the extent of the contributions of these three noise sources.

3.8.1 Preliminary Test I (Engine + Tire + Exhaust)

Prior to the test, the transmission parameters were used to find the running conditions regarding the pass-by noise requirements. The gear ratio and final drive ratio of the vehicle were utilized together with the tire circumference value, and the values of RPM which correspond to the range of the operating speed were calculated. Then, the vehicle was positioned on the rollers and was operated. A microphone was positioned as shown in Figure 3.11 for recording the emitted noise from the vehicle. Also, another channel was used to record the RPM signal coming from engine of the vehicle to find the virtual speed of the vehicle. By integrating the calculated speed data; the virtual position of the vehicle was calculated as well.

The vehicle was operated in both second and third gears during the tests. LMS Test Lab was utilized for both data acquisition and analysis. A band-pass filter with a pass band from 50 Hz to 10000 Hz was applied to eliminate unwanted signals. Data recording was made with a sampling frequency of $f_s = 25600$ Hz.

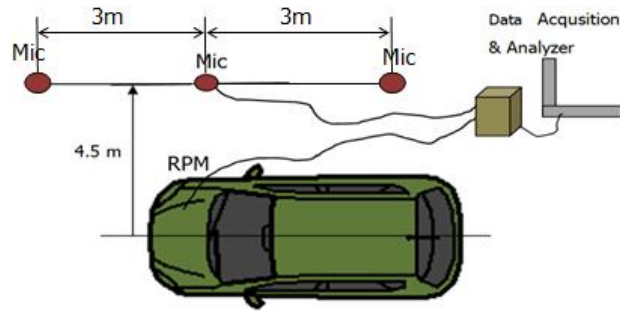


Figure 3.11 Test Setup

In the case of second gear, it can be said that the overall sound level is mainly controlled by $f=125$ Hz octave band from $U=50$ km/h to $U=58$ km/h speed. These correspond to 3750 RPM and 4350 RPM with a total transmission ratio of $r_{total}=8.53$. Apart from this band, there is no distinctive frequency which is regarded as to be dominant. On the other hand; starting from $f=400$ Hz and ending at around $f=4000$ Hz, it can be said that the acoustic pressure signal has tonal certain components though not so distinct as the one at 125 Hz. (Check Figure 3.12)

In the third gear, the dominant tonal behavior is found to shift down to 79 Hz. It is due to the lower RPM values which vary between 2400 RPM and 2750 RPM with a total transmission ratio of $r_{total}=5.67$. The characteristics for this signal is almost the same as the second gear; but at 1000Hz the tonal appearance is regarded to be the second dominant frequency band which is related to the tire noise. (Check Figure 3.13)

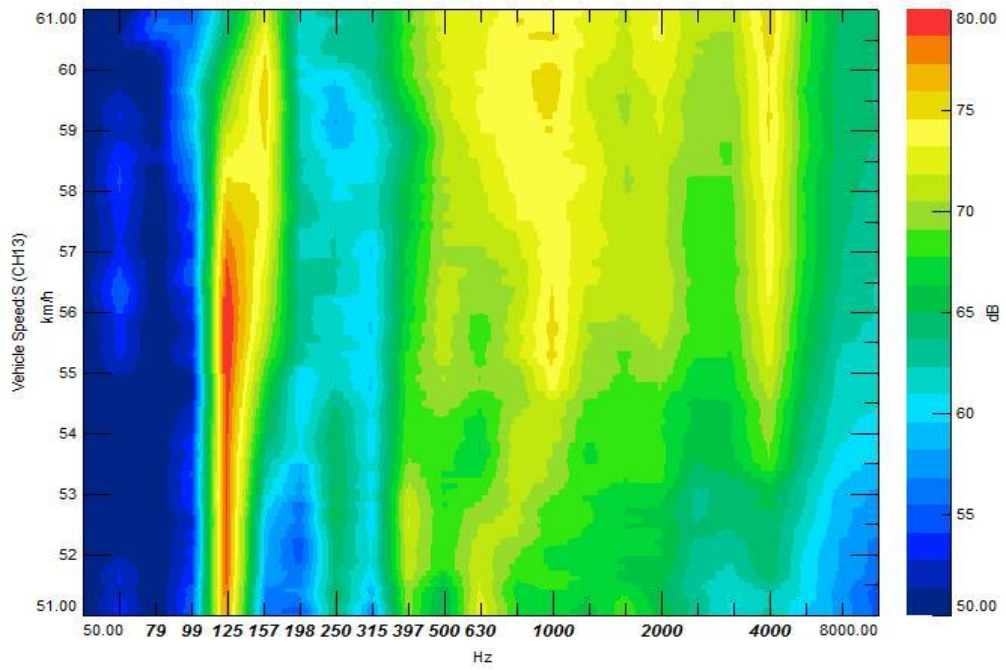


Figure 3.12 Frequency Spectrum for Second Gear between $U=50\text{km/h}$ and $U=61\text{km/h}$

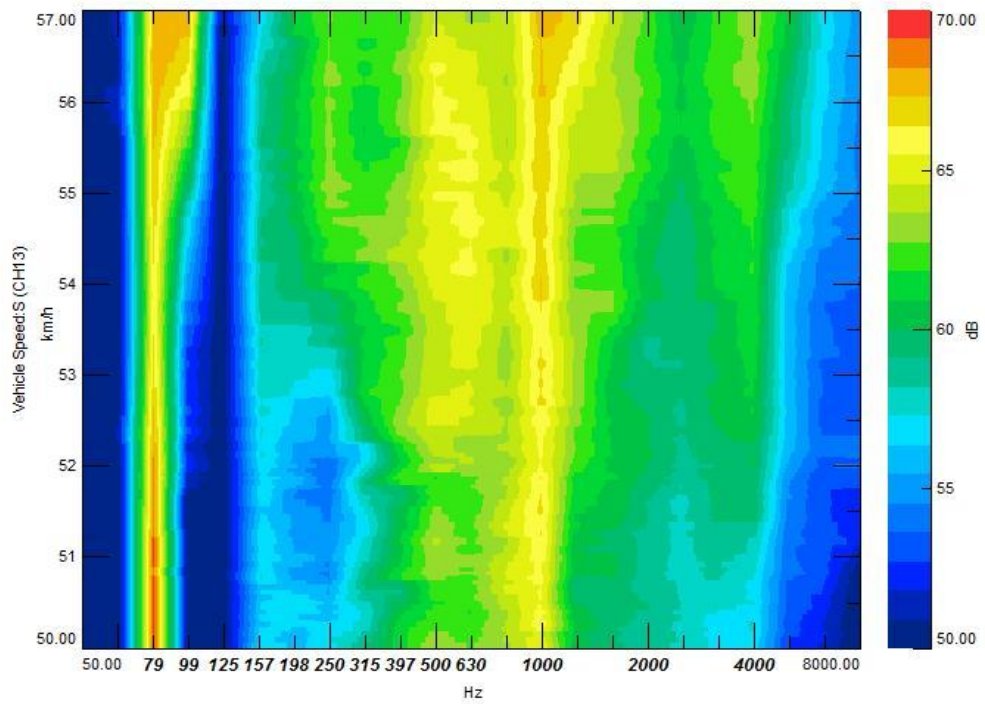


Figure 3.13 Frequency Spectrum for Third Gear between $U=50\text{km/h}$ and $U=57\text{km/h}$

When the ratio between the RPM values which are 2400 Hz and 3750 Hz for second and third gear is checked, it can be clearly seen that it is the same ratio between $f=79$ Hz and $f=125$ Hz. This information shows that the dominant frequency bands for the two gears are closely related to the RPM values.

3.8.2 Preliminary Test II (Induced Exhaust Noise)

In the second test, a similar test set up was prepared as shown in Figure 3.11. In addition, two microphones were added to gather information according to the different positions. Two cases were investigated. Firstly, the vehicle is operated as in the first test above. Secondly, an additional silencer is mounted to the exhaust orifice so as to suppress the exhaust noise as much as possible. The resulting noise levels are plotted with respect to the virtual vehicle position which is derived from the RPM signal.

Measurements were taken for both second gear and third gear. The vehicle was fully throttled by a driver as in the standard procedures. In the following figures; L_A values recorded by three microphones are given with four different lines which correspond to two cases for each gear.

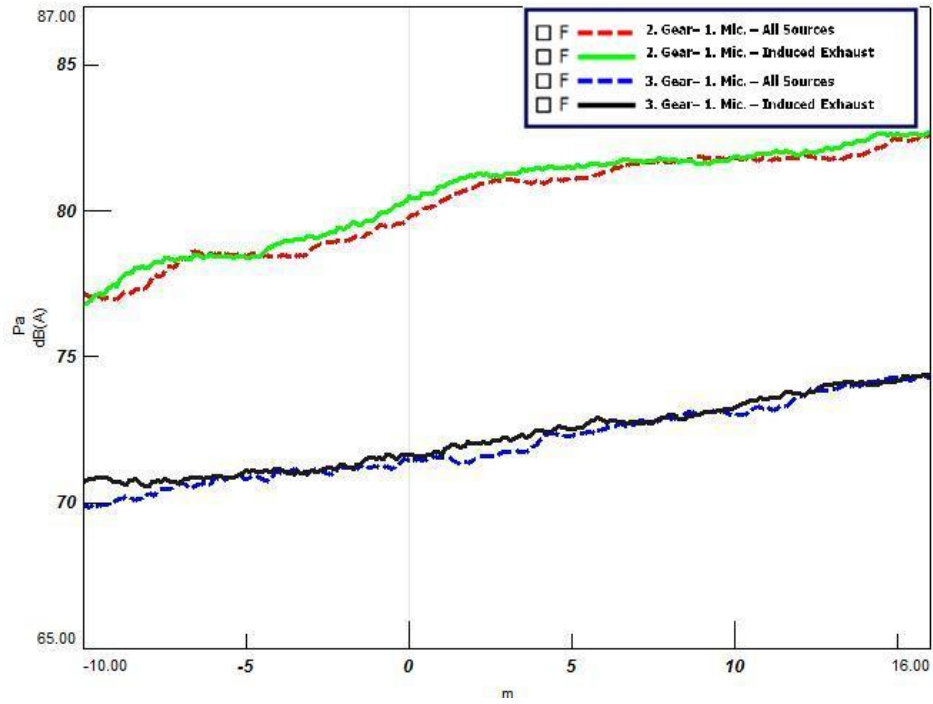


Figure 3.14 Mic-1 L_A Values for 2. and 3. Gear Tests

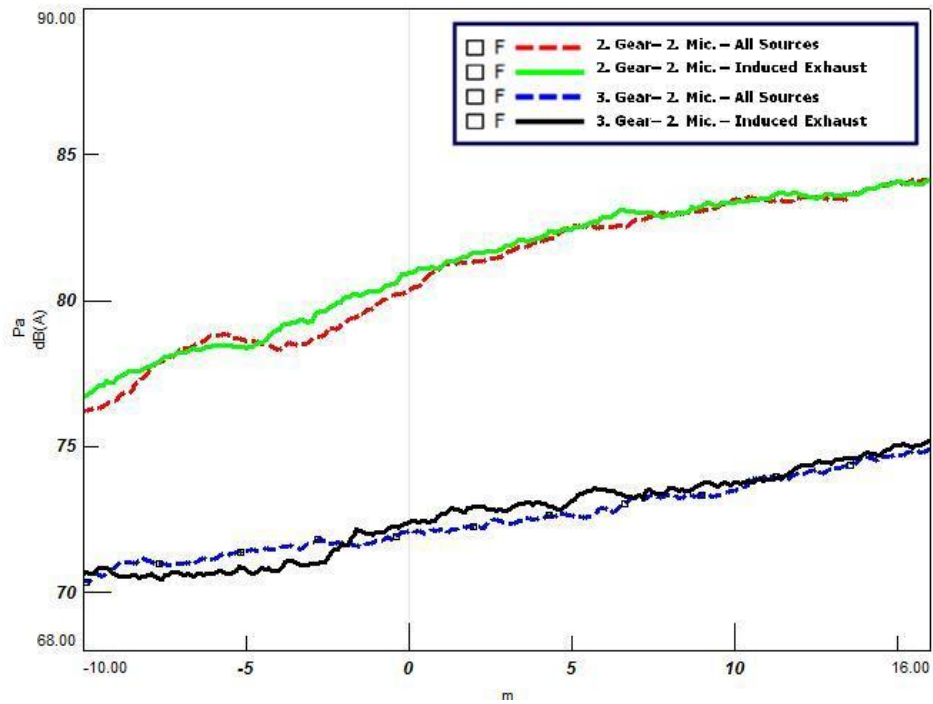


Figure 3.15 Mic-2 L_A Values for 2. and 3. Gear Tests

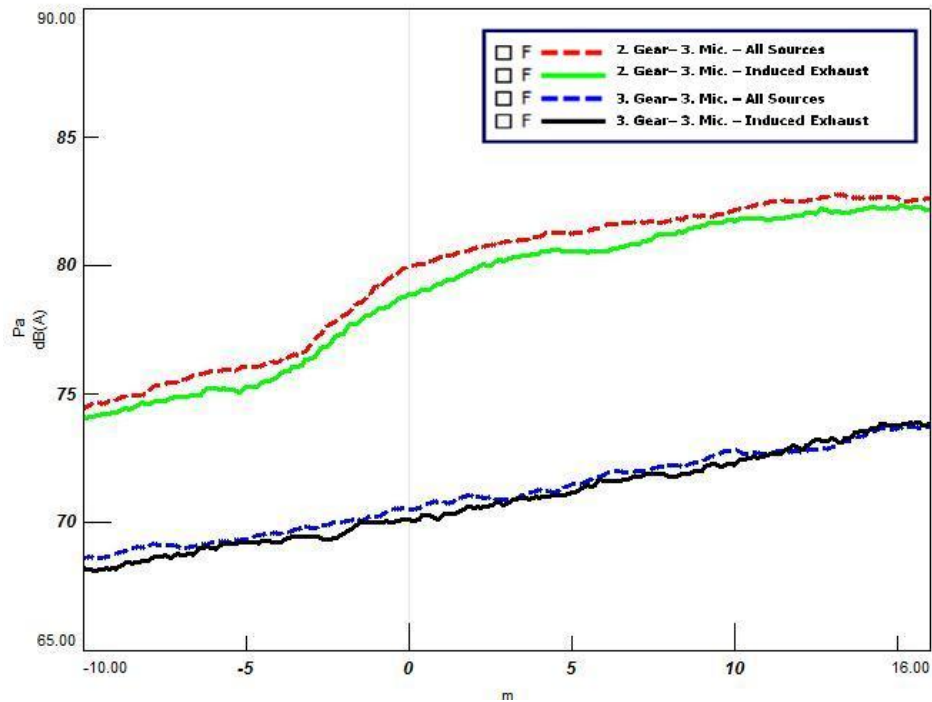


Figure 3.16 Mic-3 L_A Values for 2. and 3. Gear Tests

When these figures (Figure 3.14, Figure 3.15 and Figure 3.16) are investigated, it can be said that the contribution of exhaust orifice noise can be neglected. Especially, in the third gear (higher gear), since the speed of the engine (RPM) is lower, the sound pressure level of exhaust outlet at the measured distance is very small in comparison to the overall level. Thus, it can be generalized that the contribution of exhaust orifice can be neglected according to these preliminary tests.

3.8.3 Preliminary Test III (Tire Noise)

The measurement setup shown in Figure 3.11 was utilized to display the frequency spectrum of tire noise and to assess its contribution to the overall vehicle noise. The engine of the vehicle was not operating in this

test. The tire speed was set to 50 km/h, 55 km/h and 60 km/h progressively from the chassis dynamometer. Noise spectra was measured in terms of 1/3 octave band analysis as shown in Figures 3.17 to 3.19 corresponding to these speeds. The overall A-weighted level was also recorded for three cases. Since all of the microphones had similar noise spectrum characteristics, the second microphone was chosen as a reference. The related figures are below.

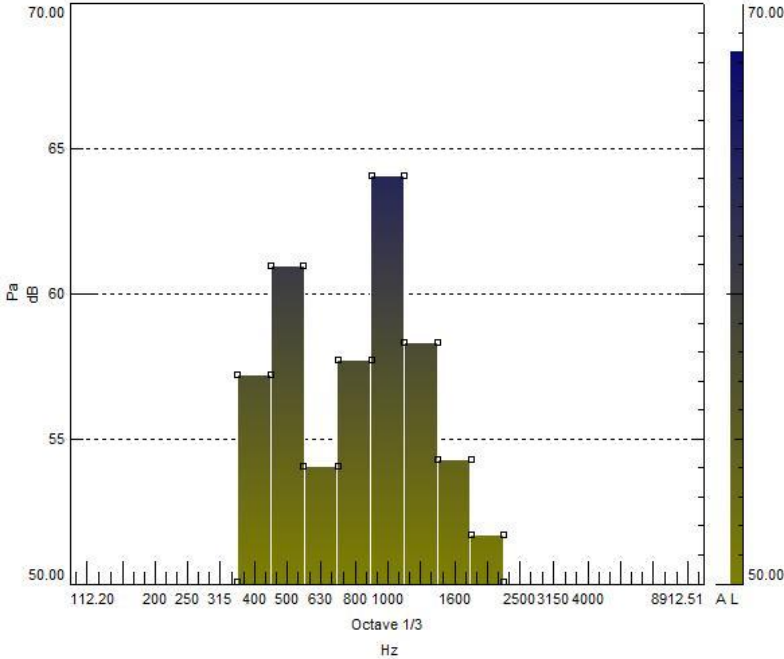


Figure 3.17 1/3 Octave Noise Spectrum at U=50km/h

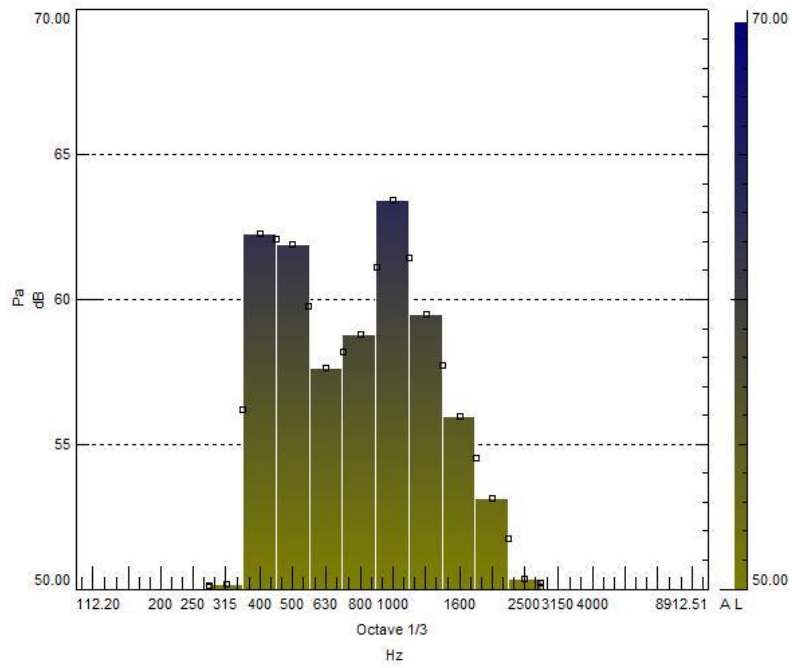


Figure 3.18 1/3 Octave Noise Spectrum at U=55km/h

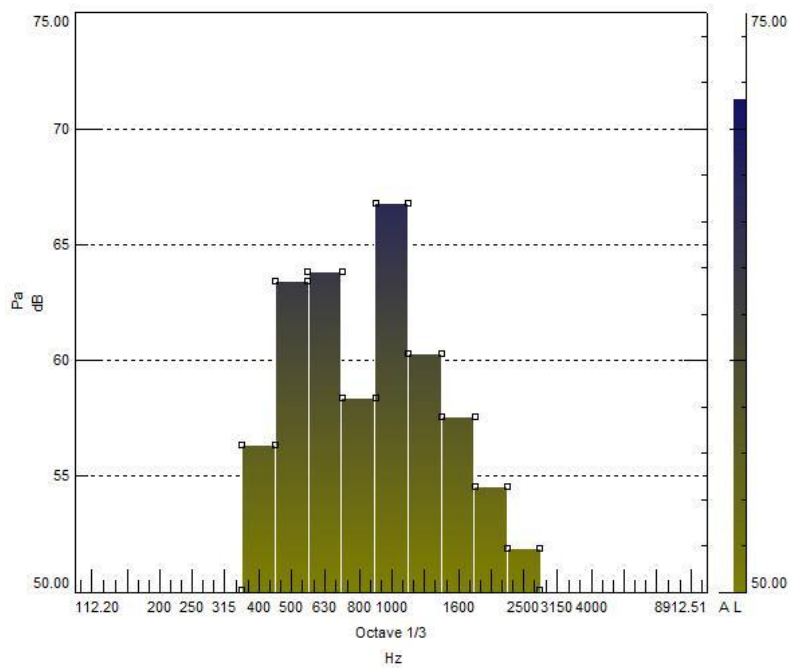


Figure 3.19 1/3 Octave Noise Spectrum at U=60km/h

When the above figures (Figure 3.17, Figure 3.18 and Figure 3.19) are inspected, it is obvious that the dominant frequency component of tire noise at three different speeds lies in 1000 Hz band. 500 Hz band can also be regarded as an emphasized component although its contribution is not as high as that of 1000 Hz band. It can be seen from the overall sound levels that there is a +3 dBA difference between 50 km/h and 60 km/h speeds at the microphone position. This information will be interpreted and utilized in the proposed method.

When the overall sound level is checked, it can be seen that the tire noise has SPL values changing from 68 dBA to 71 dBA at the specified location. And, if those values are compared to the values of the prior tests regarding the whole vehicle (engine + tire + exhaust) noise, it can be noted that the effect of tire noise is very high in the third (higher) gear; especially at around 1000 Hz band.

3.9 Investigation of Vehicle Noise Propagation over Asphalt Ground

The case of true spherical divergence in which L_p drops 6 dB for every doubling of distance does not respond to the outdoor situation. Reflections from the earth generally tend to make the L_p drop less than 6 dB. In literature, the attenuation value is suggested to be taken close 4 dB rather than 6 dB per doubling the distance [7, 11].

Since the vehicle pass-by noise measurements are described in standards for outdoor testing in which the vehicle is required to be driven on the asphalt ground, the vehicle noise propagation due to distance should be investigated. For this purpose, outdoor test setup was prepared and Fiat Doblo was used as in the prior tests. Six microphones were utilized. Three of the microphones were positioned in the line which is 4 m away from the

vehicle centerline and the other three were positioned on the line at 7.5 m away from the centerline as in Figure 3.20.

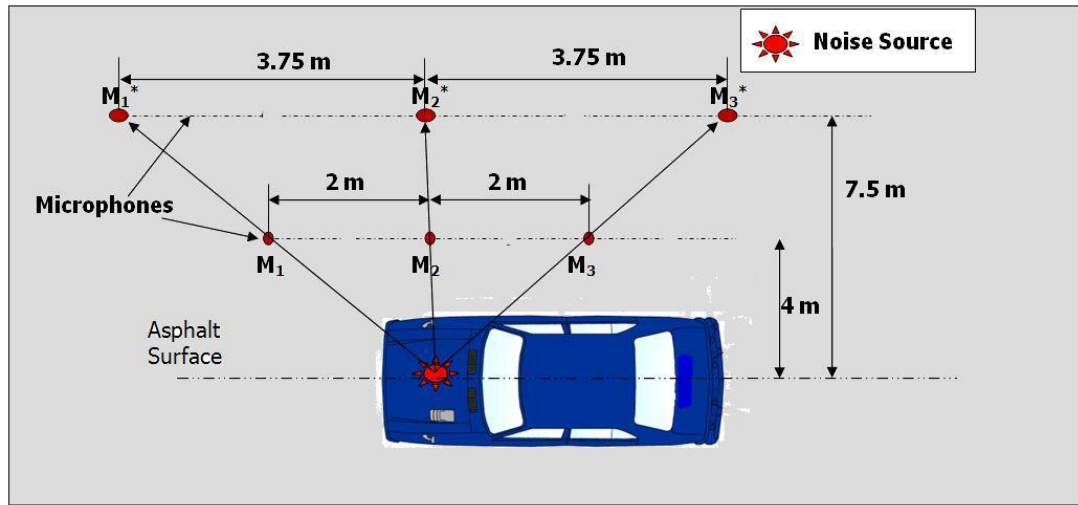


Figure 3.20 Microphone Positions in Outdoor Test

The vehicle was stationary while the engine was operated idle for two different RPMs. In this case, the primary noise source was regarded as engine noise including air intake and exhaust system. Thus, the second set of microphones at 7.5 m line was positioned accordingly by assuming the noise is dominantly coming from engine position (see Figure 3.20).

If the below results are checked, it can be seen that sound attenuation values are similar for both RPM's. Since the distance ratio has a value of 1.875, the attenuation level is expected to be 5.6 dB for true spherical spreading. However, this approximation does not fit the outdoor case. The attenuation levels calculated from the measurements are given in Table 3.3. It can be clearly stated that the attenuation levels indeed varies between 5.2 dB and 3 dB regarding to the position of microphones. Especially, in the region between engine block and the rear of the vehicle, sound attenuation levels are rather lower than the value for true spherical case.

Table 3.3 Attenuation Values for corresponding Microphones for Outdoor Test

		3100 RPM	4500 RPM
Position	Microphones	Attenuation Level (dB)	
Front	M ₁ (at 4 m) and M ₁ * (at 7.5 m)	5.2	5.2
Middle	M ₂ (at 4 m) and M ₂ * (at 7.5 m)	4.5	4.3
Rear	M ₃ (at 4 m) and M ₃ * (at 7.5 m)	3	3
Average		4.2	4.2

3.10 Simulation Model of Indoor Pass-by Noise

In this section, pass-by noise simulation procedures of a traditional four-stroked automobile will be explained in a rational framework. According to the results of preliminary diagnostic tests outlined above as well as the related studies in literature, the vehicle noise is proposed to be modeled as composed of three acoustic sources which are engine noise including air intake noise, front tire noise and rear tire noise.

3.10.1 Microphone Positioning and Measurements

The available semi-anechoic room at TOFAŞ does not satisfy the required inner dimensions. A prediction method has to be developed to adopt the under dimensioned test facility for the estimation of sound

pressure levels at 7.5 m away from the vehicle centerline on each side. The sound pressure data of the vehicle is to be acquired by series of microphones which are positioned on parallel lines to the vehicle, as shown in Figure 3.20. The main advantage of using this microphone set up rather than several microphones each of which is positioned very near to acoustic sources (engine, tires, etc.) is to collect information about the directivity of the radiated sound pressure. The distance of 4 m is chosen due to the limits regarding the room dimensions. The spacing between the microphones is taken as 1 m which can be regarded to be sufficient to have quite a detailed resolution for pass-by noise prediction. This configuration does not require more than 14 microphones.

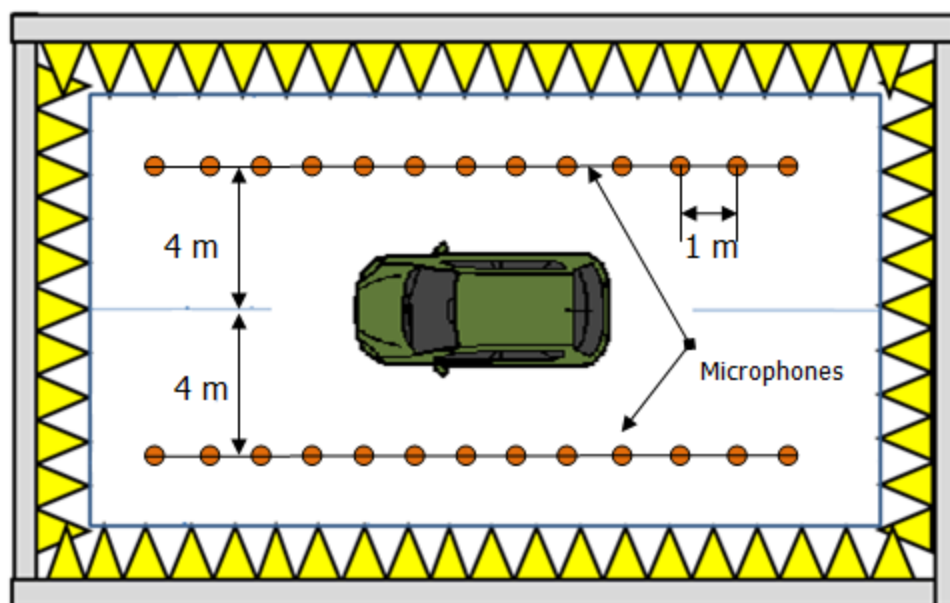


Figure 3.20 Microphone Configurations

As the first step, tire noise measurements can be done by simply operating the front tires from the chassis dynamometer console. The speed performance of the tested vehicle during pass-by noise measurements according to the ISO 362 can be calculated by using a simple formulation

and vehicle parameters (gear and final drive ratios, tire radius). Generally, as depicted in the standards, the speed of the vehicle varies from 50 km/h to 60 km/h during the test. Stationary recordings with the microphones are realized while operating the tires at different speeds like 50 km/h, 55 km/h and 60 km/h. Then, these sets of measured data will be used to form a function of tire noise with respect to the vehicle speed or virtual (derived) vehicle position by simply combining the L_A values at required speed from corresponding microphones. After modeling the front tire noise with respect to the position or speed of the vehicle, virtual rear tire noise source can be modeled using this information. Sound pressure contribution by rear tires will be taken as the same as that of front tires. However, the only difference is that the contribution will be a shifted version of the contribution by front tires to account for their position.

Two more channels which contain RPM signal and throttle information are required for the measurement of the complete vehicle noise. The data coming from these channels are used as control parameters in the test. A sensor is mounted just under the gas pedal which sends signal when the vehicle is fully throttled by the driver. Just when the vehicle/engine speed is at the starting value, the driver fully throttles the vehicle and the measurement process starts. The measurement can be stopped manually when the RPM of the engine exceeds the finish point which corresponds to the virtual (derived from the RPM data) vehicle position at +10 m.

Tire noise has to be subtracted from the measured data to obtain the L_A values for engine noise (including air intake and transmission noise) only. This process can be done easily by using the fact that they are incoherent. Thus, the engine noise can be obtained by simply subtracting the sound pressure level of tire noise which was acquired as function of vehicle speed or vehicle position from the overall sound pressure level measured in the second test.

3.10.2 Sound Divergence due to Distance

After obtaining the data from the above measurements at 4 m for each noise source and processing them as L_A functions with respect vehicle speed or position, sound attenuation calculations due to distance are done in accordance with the illustration in Figure 3.21.

For each of the noise source, this analytical model is adopted by considering their positions on the vehicle. As it can be seen from the figure, the ratio due to distance " r_2/r_1 " will be same. Here, r_1 is the distance between the noise source and measurement point and r_2 is the distance between the noise source and the corresponding prediction point.

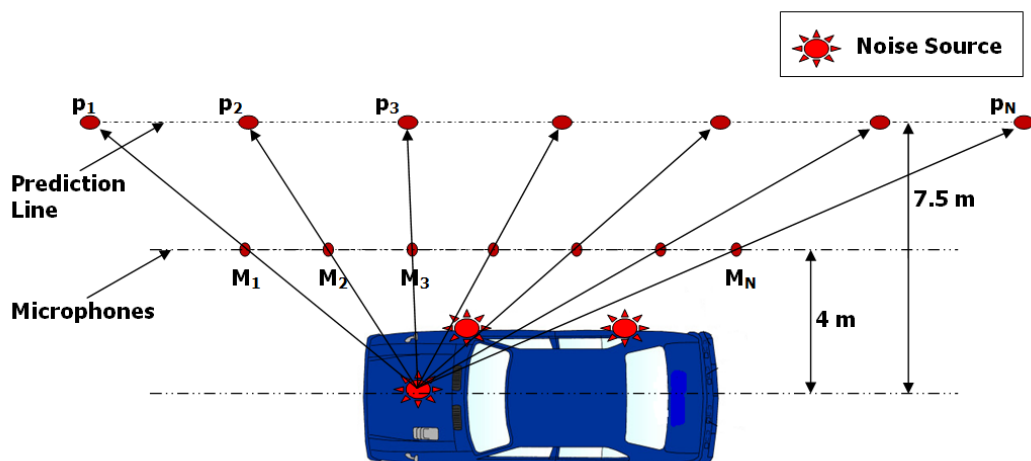


Figure 3.21 Illustration of Sound Pressure Divergence due to Distance

For example, the measured sound pressure data for engine noise at position M_1 , corresponds to the data at position p_1 which is the point on prediction line at 7.5 m away from the centerline of the vehicle. This means, with a microphone spacing of 1 m, no more than 14 or 15 number of microphones will be needed for analyzing one side of the vehicle.

3.10.3 Simulation Model

A simplified approach shown in Figure 3.22 can be pursued after acquisition of the measurement data from the indoor measurements. A simulation of sound propagation regarding the distance between the sound sources (engine, front and rear tires) and microphone position at 7.5 m is modeled. It is mainly consisted of four stages as

- 1- Sound attenuation due to the distance and reflection,
- 2- Time delay due to the distance,
- 3- Doppler shift due to the vehicle motion with respect to the fixed microphone
- 4- Superposition of calculated L_A functions.

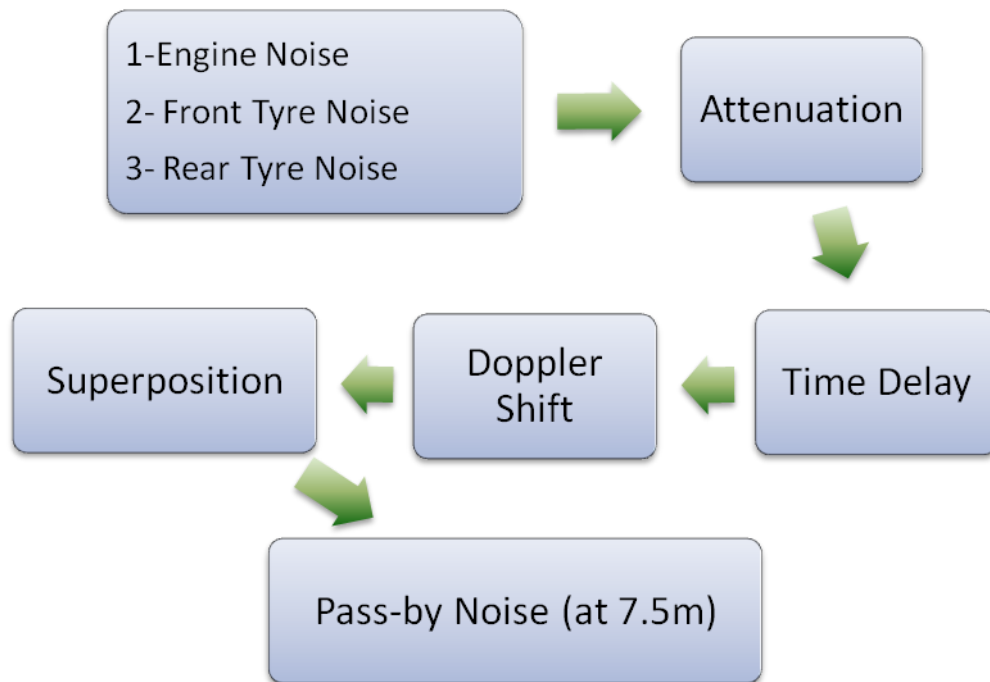


Figure 3.22 Simulation Model for Indoor Pass-by Noise

Measured sound pressure levels at the distance ($d=4$ m in this case) smaller than 7.5 m are propagated to transfer from 4 m to 7.5 m according to the distance from the sources. Estimations and calculations are to be done with respect to point sources and line sources since analytical solutions for noise radiated into free field from arbitrarily shaped vibrating structures are not available.

When modeling the sound pressure attenuation due to distance, spherical sound divergence is not taken as 6 dB per doubling the distance. According to the former outdoor and indoor tests and information in literature [11], sound pressure attenuation per doubling the distance is taken as 4.2 dB. This is because the pass-by noise measurements are done outdoors where it does not satisfy true spherical divergence. However, this value is to be validated for other semi-anechoic chambers since they may have different acoustical characteristics.

A time delay or transport lag occurs due to the distance between the sources and microphones. In other words, a signal that is emitted by the source at time $t=t_e$ is perceived at the microphone position at time $t=t_r$. If the instantaneous distance is denoted by " ΔR ", then the relation can be expressed as;

$$t_r = t_e + \frac{\Delta R}{c_0} \quad (3.27)$$

Here, c_0 is the speed of sound in the medium. It should be noted that ΔR is the distance at $t=t_e$ emitted time.

Other important phenomena are Doppler Effect and ground reflections. Doppler Effect leads to amplitude and shifts the signal frequency depending on the relative motion between the source and the receiver. If the formula

for sound radiation of a moving point source is associated with the image source formula derived for ground reflections, it becomes [57];

$$P = \frac{\dot{Q}\left(t - \frac{R}{c}\right)}{4\pi R(1 - M\cos\theta)^2} + \frac{Q(\cos\theta - M) \cdot u}{4\pi R^2(1 - M\cos\theta)^2} + \frac{\dot{Q}_i\left(t - \frac{R^i}{c}\right)}{4\pi R^i(1 - M\cos\check{\theta})^2} + \frac{Q_i(\cos\check{\theta} - M) \cdot u}{4\pi R^{i^2}(1 - M\cos\check{\theta})^2} \quad (3.28)$$

Here, \dot{Q}_i is the sound strength of the image source and R^i is the position vector from image source to the receiver point. From this equation, the amplitude correction factor can be evaluated as,

$$K_{Amp} = \frac{1}{(1 - M\cos\theta)^2} \quad (3.29)$$

After computing the L_A values with respect to the vehicle position for engine, front tire and rear tire individually using the above simulation procedures, superposition (summation) process is done and the predicted pass-by noise level can be acquired. More detailed flowcharts of the acoustical simulation model are given in Appendix C.

CHAPTER 4

EXPERIMENTAL AND SIMULATED RESULTS

4.1 Definition of the Measurements

Based on the simulation model developed in Chapter 3, pass-by noise prediction processes were applied on two different types of vehicles. The specifications of the vehicles are given in Table 4.1.

Table 4.1 Vehicle Specifications

Parameters	First Vehicle	Second Vehicle
Vehicle Type	FWD light commercial, front-engine	FWD passenger, front-engine
Maximum Power	75 hp	110 hp
Fuel Type	Diesel	Diesel

Firstly, the measurements were made on the first vehicle. The test set up is shown in Figure 4.1. Nine microphones were positioned parallel to the vehicle and they were located four meters away from the centerline towards the right side. The spacing between the microphones is taken equal to one

meter. Arrangements were made to obtain the vehicle speed data and throttle data as described above.



Figure 4.1 Measurement Configuration for the First Vehicle

The same measurement set up was configured for the second vehicle (Figure 4.2). The number of microphones was increased. Two more microphones were positioned to the front and one additional microphone was settled in the back of the array.



Figure 4.2 Measurement Configuration for the Second Vehicle

ISO 362-2007 was taken as a reference for pass-by noise measurement procedures. According to this; speed and acceleration profiles of the vehicles are taken as;

- Vehicle speed should be 50 km/h at the start line where vehicle position is -10 m,
- Vehicle is fully accelerated at the start line in two different gears (2. and 3. Gears)

LMS Scadas system was utilized for recording and triggering. It has a capability of sixteen slots for transducer inputs and two slots for tacho data. Technical properties of Scadas systems can be found in Appendix-C. LMS TestLab software was also used for digital signal processing. The acquisition parameters were defined into the software through user console.

The virtual speed of the vehicle is calculated using the formula;

$$U_{vir} = \frac{RPM * 60 * P_T}{Ratio_{gear} * Ratio_{final} * 1000} \quad (4.1)$$

Here; P_T is the circumference of the tire, $Ratio_{gear}$ is the gear ratio and $Ratio_{final}$ is the gear ratio of the final drive of the vehicle. And the virtual position can be derived as;

$$X_{vir} = \int U_{vir} dt - 10m \quad (4.2)$$

Using these formulations, the triggering of the measurement is done with respect to two parameters which are the vehicle speed data and the throttle signal (Figure 4.3). When the speed of the vehicle is 50 km/h at the specified gear, vehicle should be fully throttled so that the measurement is valid.

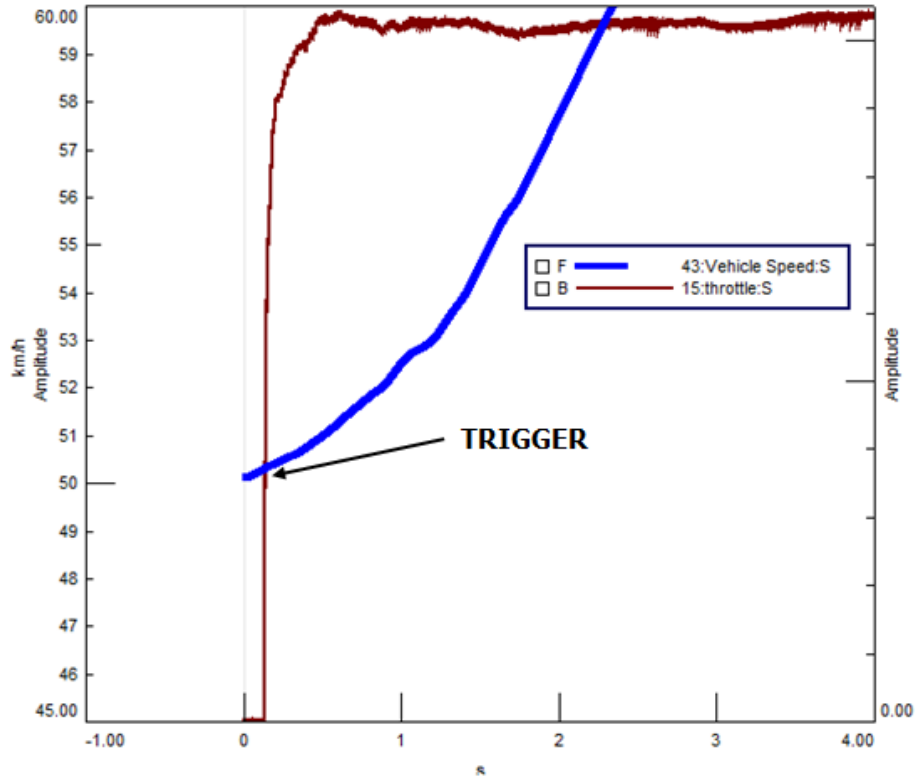


Figure 4.3 Throttle and Vehicle Speed Check (Valid Run)

4.2 Simulation Results and Comparison

The recorded time series data of the noise is firstly processed in LMS TestLab software. A band-pass filter of 50-10000 Hz was set to avoid unwanted data. The sampling frequency was chosen as 25600 Hz and Hanning Window was applied. Finally, the processed data was imported into Matlab software where the calculations and simulations were performed.

4.2.1 Results

In Matlab environment, pass-by noise prediction process was performed as defined in the previous chapter.

4.2.1.1 Results- First Vehicle

The measurements were made only for the right side of the vehicle. L_p 's are A-weighted as depicted in the standards. The predicted pass-by noise level is given together with the individual sound sources which are the engine noise, front and rear tire noise. As it can be seen from Figure 4.4 and Figure 4.6, the tire noise is higher in the case of the third gear where the RPM of the engine is lower compared to the second gear.

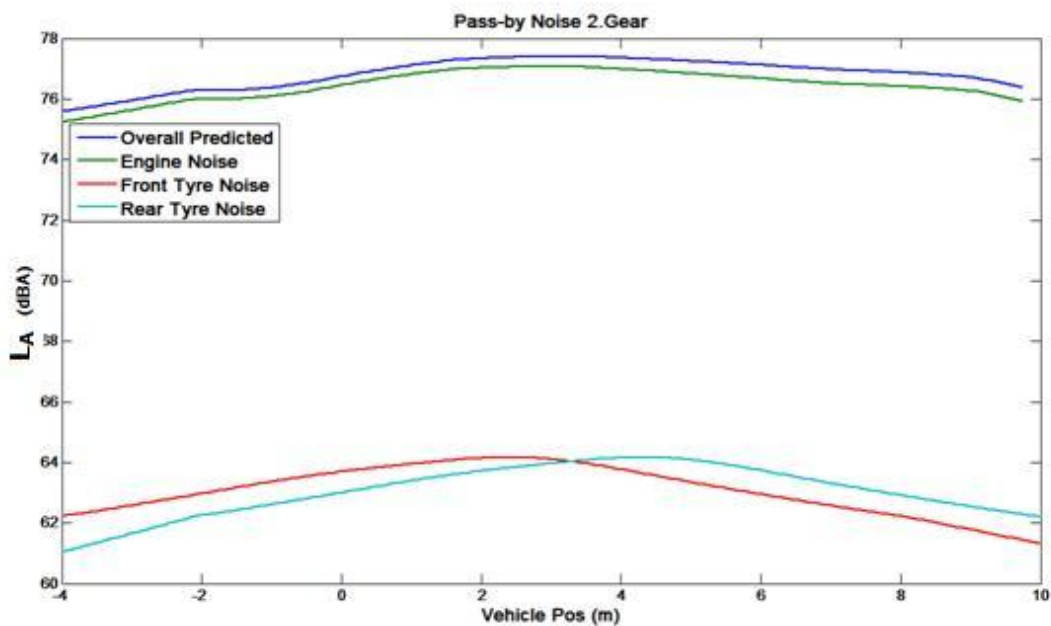


Figure 4.4 L_A Values for Predicted Pass-by Noise, Engine Noise and Tire Noise for 2.Gear

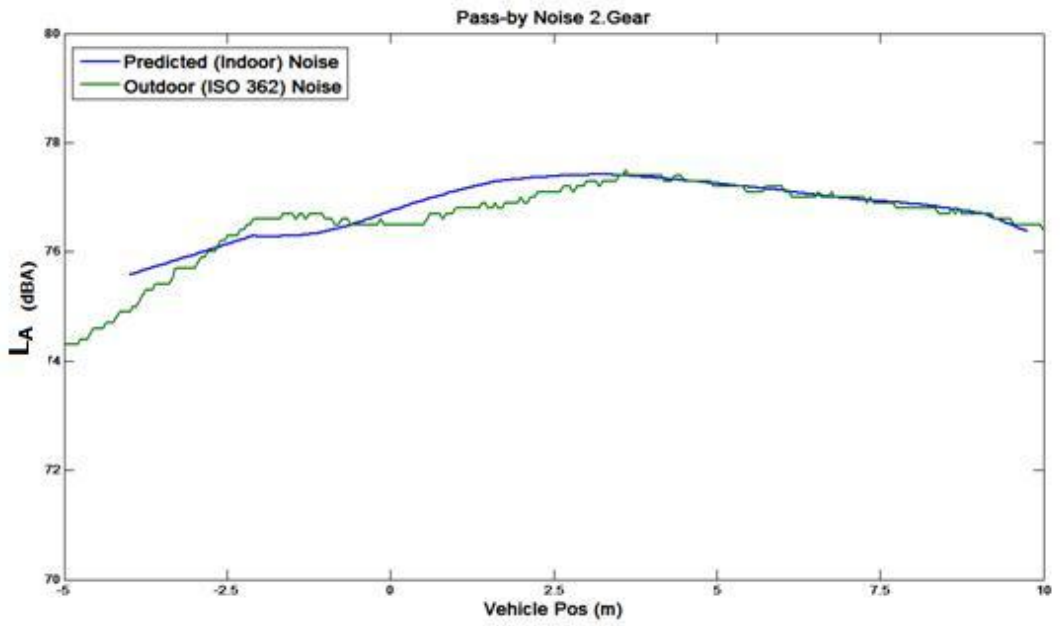


Figure 4.5 Comparison of Predicted (Indoor) and Outdoor (ISO 362) Pass-by Noise Levels

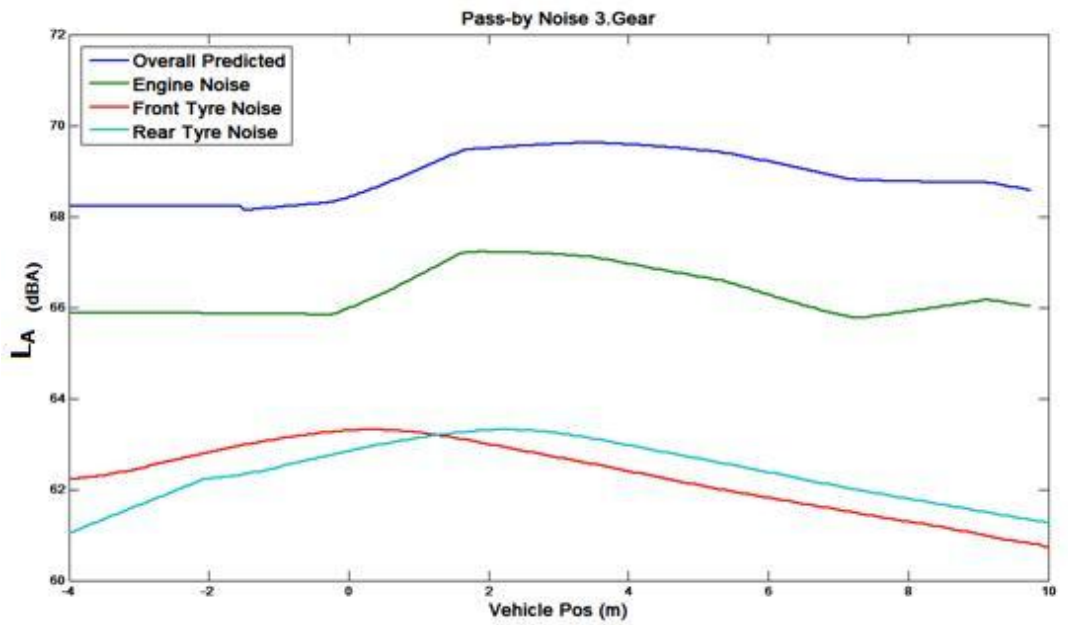


Figure 4.6 LA Values for Predicted Pass-by Noise, Engine Noise and Tire Noise for 3.Gear

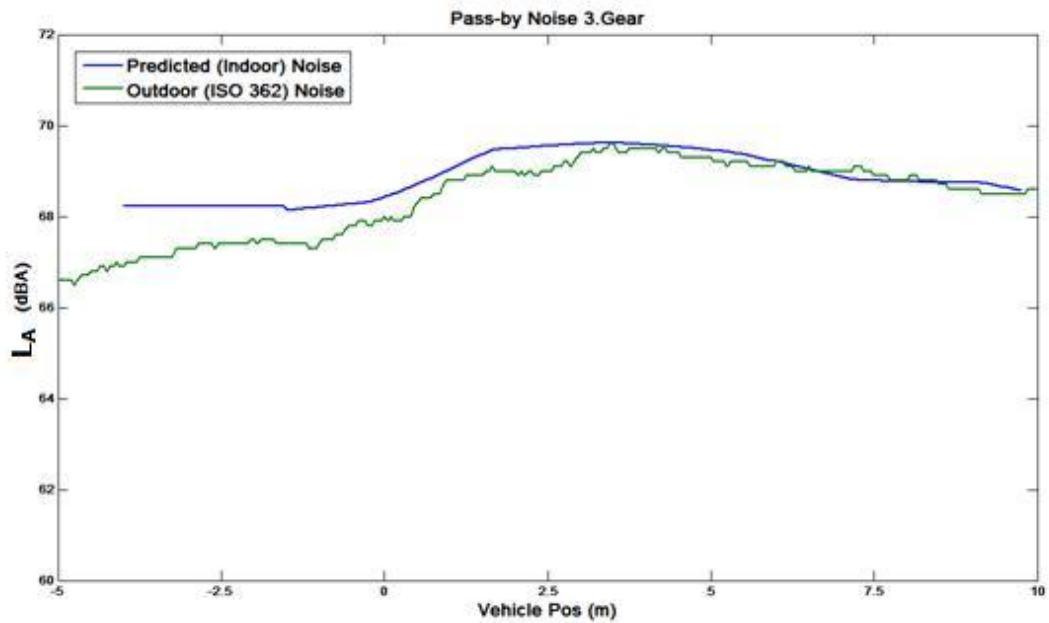


Figure 4.7 Comparison of Predicted (Indoor) and Outdoor (ISO 362) Pass-by Noise Levels

The results show that the predicted (indoor) and measured (outdoor) pass-by noise values for the first vehicle are in good agreement with each other, especially in the second half (0 - 10 m) of the vehicle position. It can be easily seen that the contribution of the tire noise in the case of the second gear measurements is very low, but still cannot be neglected.

4.2.1.2 Results – Second Vehicle

The same steps were repeated for the second vehicle. The only difference was that the number of microphones used in the measurements was increased to thirteen to cover a wider range. The same simulation model as for the first vehicle was used for predicting the pass-by noise.

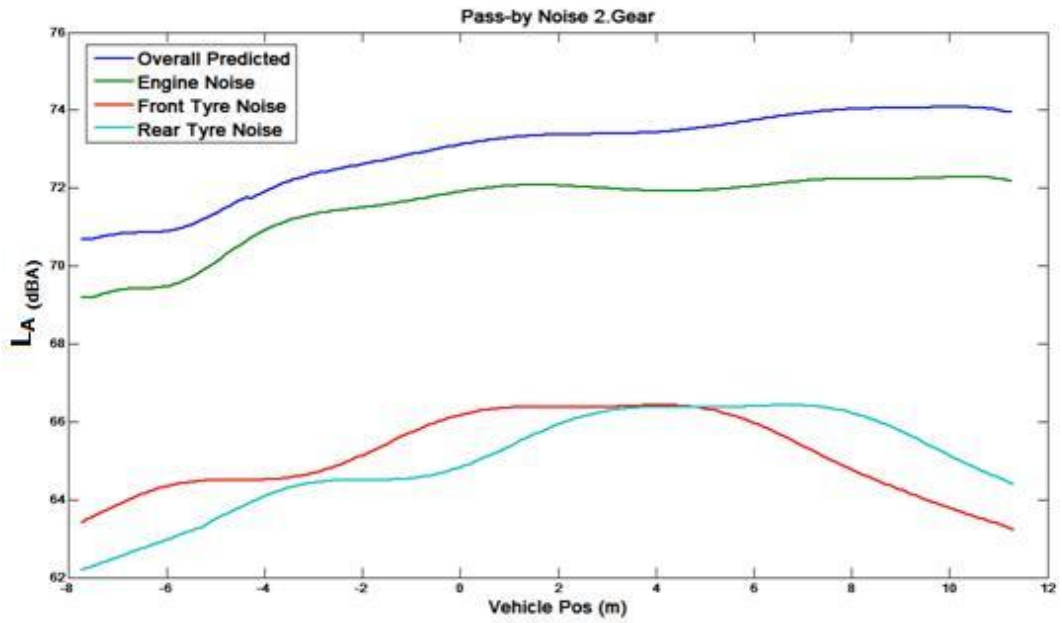


Figure 4.8 LA Values for Predicted Pass-by Noise, Engine Noise and Tire Noise for 2.Gear

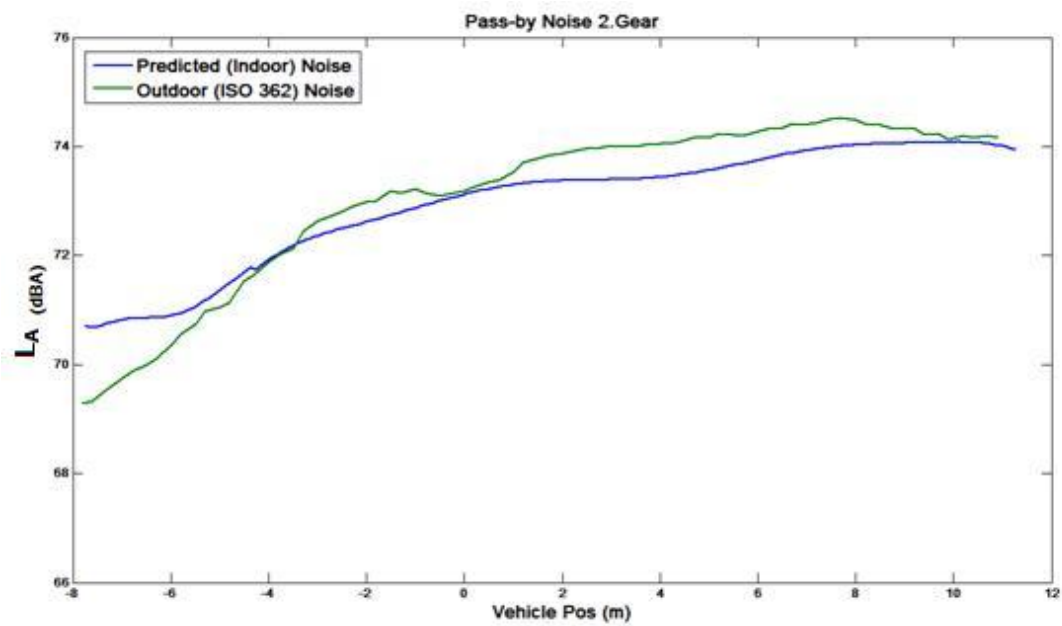


Figure 4.9 Comparison of Predicted (Indoor) and Outdoor (ISO 362) Pass-by Noise Levels

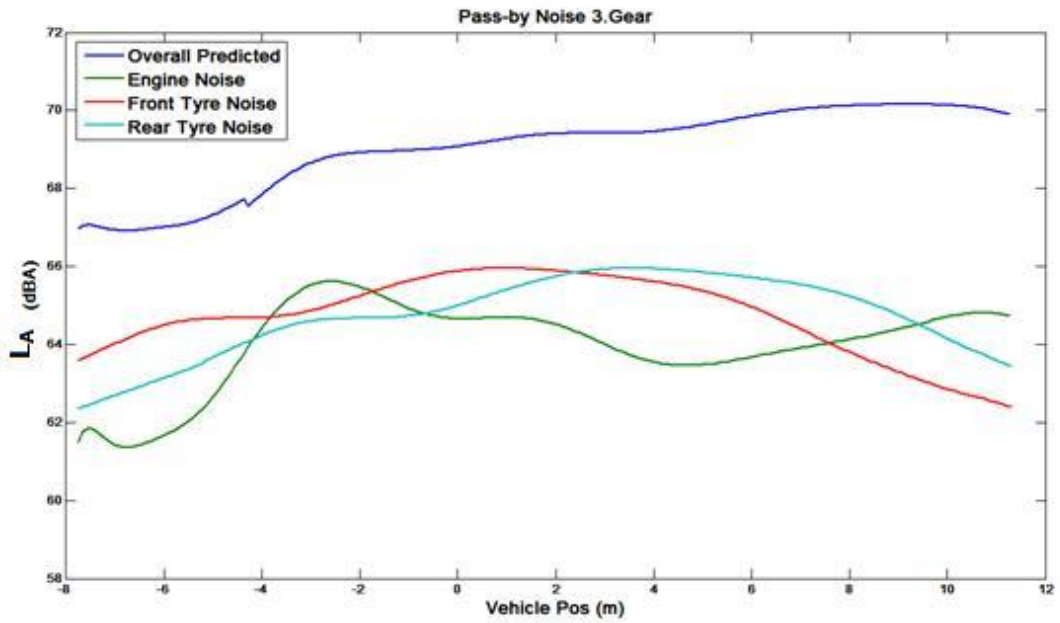


Figure 4.10 L_A Values for Predicted Pass-by Noise, Engine Noise and Tire Noise for 3.Gear

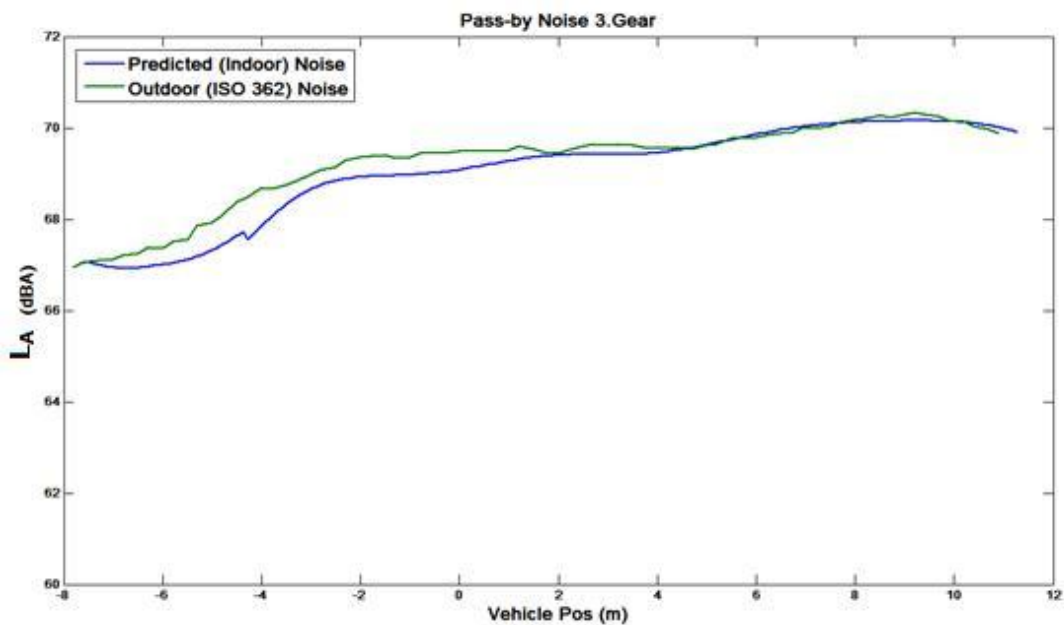


Figure 4.11 Comparison of Predicted (Indoor) and Outdoor (ISO 362) Pass-by Noise Levels

When the harmony between the outdoor (ISO 362) test results and simulation results are checked, it can be said that they match almost perfectly in the case of the third gear. Although the maximum levels which were acquired for the second gear differ from each other with a value under 0.4 dB, it can still be regarded reasonable since it is below the tolerance range of the goal (0.5 dB) and since the overall characteristics of the L_A are similar.

4.2.2 Comparison of the Results

For the purpose of comparison, commercial software was used for the prediction of the pass-by noise level of the vehicles. The software is indeed suggested to be used by the manufacturer at the exact pass-by noise measurement distance which is 7.5 m. The L_A functions acquired from both outdoor (ISO 362) tests and prediction model developed are compared in the same plot in the case of two different vehicles for two different gears. Also, Root Mean Square Errors "RMSE" for each case are discussed for overall statistical comparison.

4.2.2.1 Comparison – First vehicle

The results for the first vehicle are displayed in figures below.

Second Gear

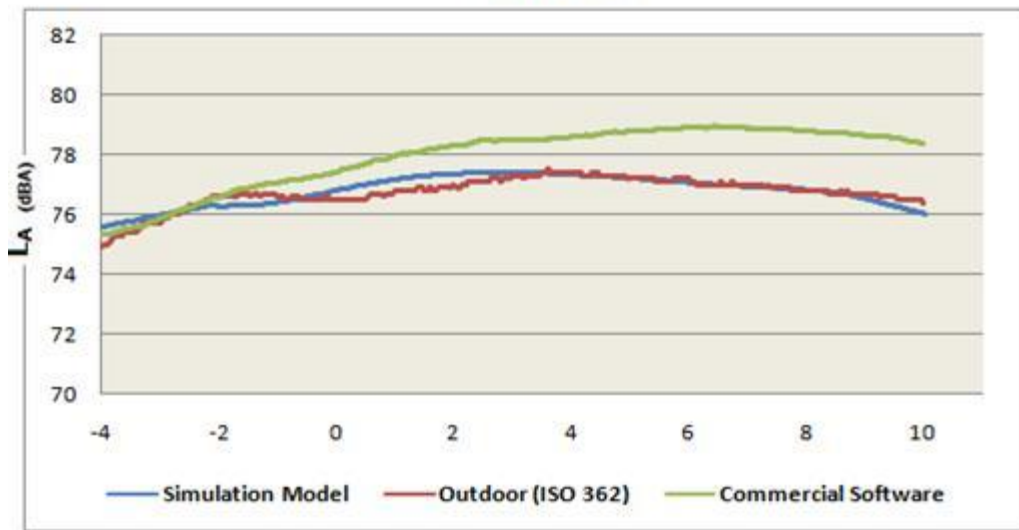


Figure 4.12 Comparison of Pass-by Noise Levels (L_A) for Second Gear

Third Gear

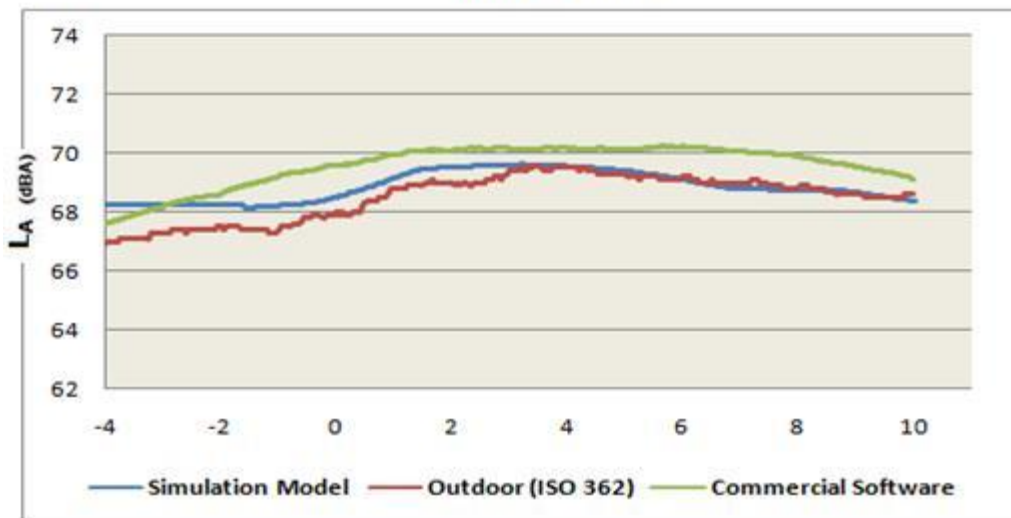


Figure 4.13 Comparison of Pass-by Levels (L_A) for Third Gear

For both second and third gear results, it can easily be seen from the figures above that simulation model yields better results than the commercial software. If the RMSE values are checked; in the case of second

gear tests, commercial software gives 1.18 dB error while the simulation model only gives 0.26 dB error. And when the third gear test results are checked, commercial software yields 0.93 dB error while the simulation model has an RMS error of 0.56 dB.

4.2.2.2 Comparison – Second Vehicle

The results for the second vehicle are illustrated below.

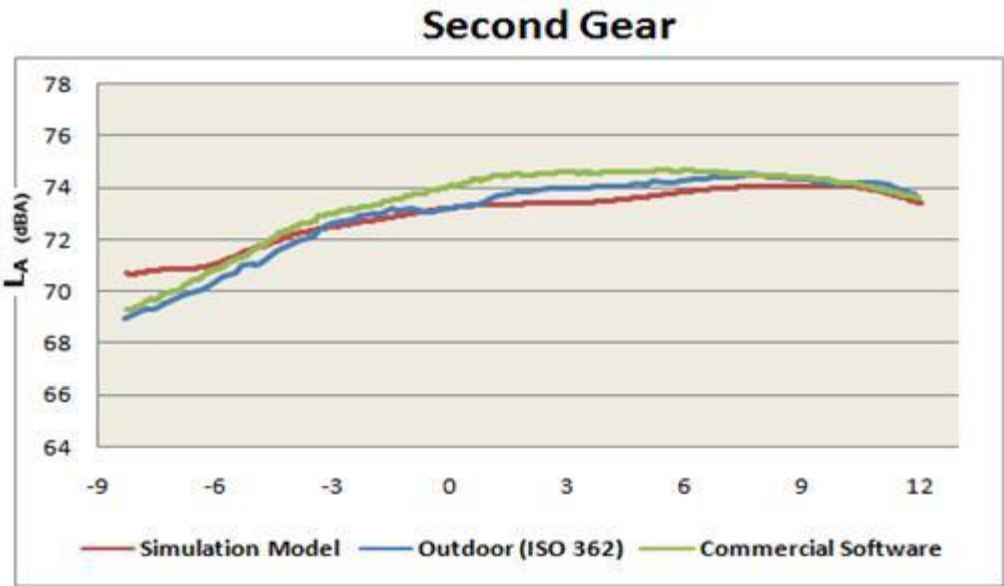


Figure 4.14 Comparison of Pass-by Noise Levels (LA) for Second Gear

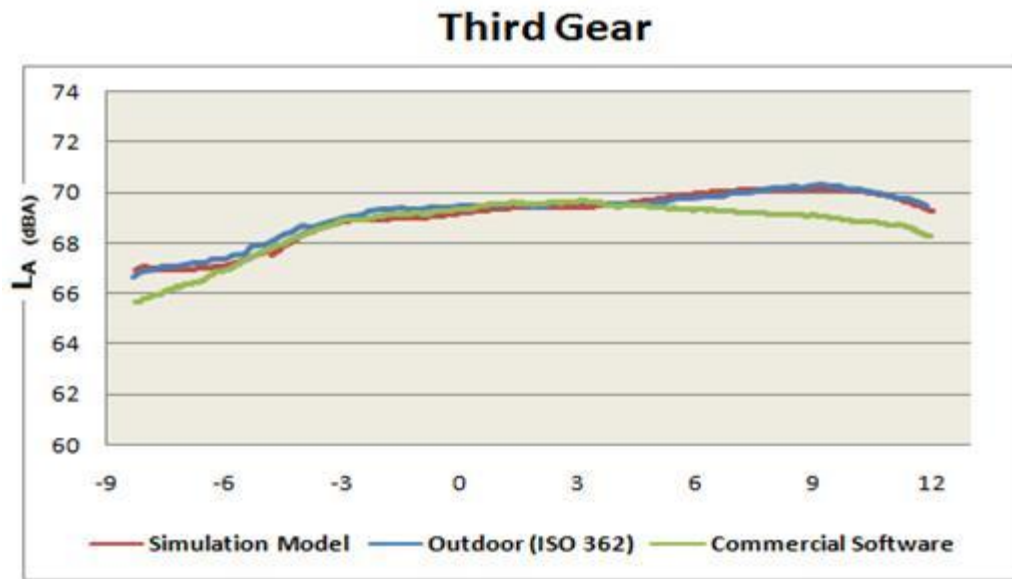


Figure 4.15 Comparison of Pass-by Levels (L_A) for Third Gear

When the second and third gear results are checked, it can be stated that the developed model is a bit more accurate overall than the commercial software. Regarding the second gear test results, the commercial software gives 0.47 dB RMS error while the simulation model gives quite the same error value, 0.45 dB. And in the case of third gear, the commercial software yields 0.67 dB error while the simulation model gives only 0.22 dB RMS error.

It can be concluded that the simulation model simulates the vehicle outdoor measurement better, since it makes a better point of the emitted noise of the vehicle from varies points; namely, engine block, front tire and rear tires.

CHAPTER 5

SUMMARY AND CONCLUSIONS

In this study, a simulation model which enables the vehicle pass-by noise measurements to be performed in a finite dimensioned, semi-anechoic room with a chassis dynamometer was developed. The developed model is able to satisfy the outdoor driving conditions such as time delay, Doppler Effect and sound reflections over road surfaces. Two different types of automobiles were used to check the accuracy between the predicted pass-by noise levels corresponding to the indoor measurements and the outdoor pass-by noise levels obtained according to the procedures defined in ISO 362.

There are some differences between outdoor and indoor pass-by noise measurements (see Section 3.6.3). To eliminate these differences and to acquire more similar pass-by noise results to outdoor measurements, assumptions and calculations were done by using the results obtained from the preliminary tests.

The vehicle was acoustically modeled as the combination of three primary noise sources which are the engine noise including air intake and exhaust, the front tire noise the rear tire noise. Sound pressure of the corresponding source was obtained by using the measurement setup shown in Figure 3.20. Since the microphones are positioned 4 m away from the vehicle centerline, this method enables the vehicle pass-by noise

measurement in a rather smaller semi-anechoic room than the one which is proposed to satisfy the outdoor test dimensions addressed in ISO 362.

After collecting the necessary data mentioned above, an acoustical simulation model was employed in Matlab environment (see Section 3.9.2). The corresponding results for the two different vehicles are given below. The results show accuracy not only in the maximum (L_A) value acquired during the test but also in the overall (L_A) behavior with respect to the vehicle position.

Table 5.1 Predicted and Measured (Outdoor) Pass-by Noise Values

		First Vehicle		Second Vehicle	
		Predicted	Outdoor	Predicted	Outdoor
2.	Max L_{Amax} (dBA)	77.4	77.5	74.1	74.5
	Gear				
	Vehicle Position (m)	3.2	3.6	9.2	7.7
3.	Max L_{Amax} (dBA)	69.6	69.6	70.2	70.3
	Gear				
	Vehicle Position(m)	3.4	3.5	9.1	9.2
Average	Max L_{Amax} (dBA)	73.5	73.6	72.1	72.4

Based on the fact that ISO 362 gives -1 dB tolerance value due to the repeatability of the pass-by noise measurement results in outdoors is not good, the results acquired in this study using the developed simulation model can be regarded as accurate and rational. However, accuracy of

results can be improved by increasing the number of microphones in the measurement setup.

The simulation model developed in this study is also capable of exhibiting the contributions of three components (engine including air intake and exhaust, front and rear tire) as well.

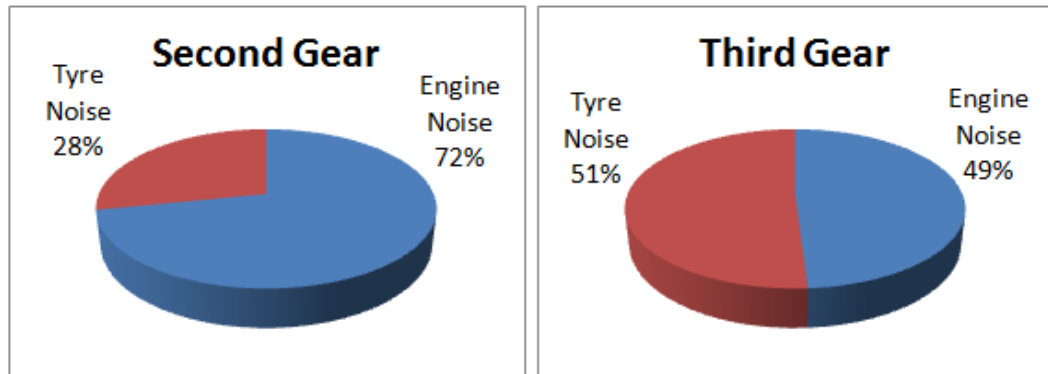


Figure 5.1 Contributions of Tire Noise and Engine Noise (including air intake and exhaust) to the Overall Pass-by Noise Level

In Figure 5.1, the average contributions of the “Tire Noise” and “Engine Noise plus Air Intake Noise and Exhaust Noise” regarding the two vehicles into pass-by noise level are shown. When the contributions of the tire (front and rear) noise and the engine (including air-intake and exhaust) noise which are taken as the principal sound sources of pass-by noise in this study are checked, it can be seen that the tire noise is almost as dominant as the engine noise in the higher (third) gear. Thus; the effect of noise coming from neither rear nor front tire cannot be neglected.

As a future work, sound attenuation level over asphalt road can be deeply investigated using more microphones and the acoustical model may be upgraded accordingly. Also, exhaust tail pipe noise can be considered as another noise component on the vehicle and the effect of this component can be checked by using the upgraded simulation model.

Car manufacturers are not only interested in maximum pass-by noise levels but also in diagnostics of exterior noise for noise reduction purposes. For this reason, future work should also be concentrated on noise source contribution analysis and deeper investigations should be done regarding exhaust noise and air intake noise. And then, the acoustical modeling of the vehicle should be extended by increasing the number of noise sources.

REFERENCES

- [1] ISO 362-1:2007, "Measurement of Noise Emitted by Accelerating Road Vehicles –Engineering Method-".
- [2] Directive 2002/49/EC, "Official Journal of the European Communities".
- [3] Directive 2007/34/EC, "Official Journal of the European Communities".
- [4] Directive 70/157/EEC, "Official Journal of the European Communities".
- [5] F. Fahy, "Foundation of Engineering Acoustics", Elsevier Academic Press, First Edition, 2005.
- [6] F. Fahy, J. Walker, "Advanced Applications in Acoustics, Vibration & Noise", Spon Press, First Edition, 2004.
- [7] D. A. Bies, C. H. Hansen, "Engineering Noise Control – Theory and Practice", Spon Press, Third Edition, 2003.
- [9] E. G. Williams, "Fourier Acoustics – Sound Radiation and Nearfield Acoustic Holography", Academic Press, First Edition, 1999.
- [9] M. Bruneau, "Fundamentals of Acoustics", ISTE, First Editon, 2006.
- [10] H. Kuttruff, "Acoustics – An Introduction", Taylor & Francis, First Edition, 2007.

- [11] F. A. Everest, P. C. Kohlmann, "Master Handbook of Acoustics", McGraw Hill, Fifth Edition, 2009.
- [12] T. D. Rossing, "Springer Handbook of Acoustics", Springer, First Edition, 2007.
- [13] M. Harrison, "Vehicle Refinement – Controlling Noise and Vibration in Road Vehicles", Elsevier, First Edition, 2004.
- [14] Y. Ban, H. Banno, K. Takeda, F. Itakura, "Synthesis of Car Noise Based on a Composition of Engine Noise and Friction Noise", IEEE International Conference on Acoustics, Vol. 2, pp. 2105- 2108, 2002.
- [15] A. R. Fleszar, P. Linden, J. R. Johnson, M. J. Grimmer, "Combining Vehicle and Test-Bed Diagnosis Information to Guide Vehicle Development for Pass-by Noise", SAE 2001 Noise & Vibration Conference & Exposition, USA, 2001.
- [16] M. Lu, M. U. Jen, "Noise Source Ranking of an All-terrain Vehicle to Meet Pass-by Target", Proceedings of Inter-Noise 09, Ottawa, Canada, 2009.
- [17] B. Kim, S. Yoo, H. Kim, K. Zwanzig, "Prediction of Vehicle Pass-by Noise Using Indoor Measurements", Proceedings of the 2001 Noise and Vibration Conference, Michigan, USA, No:1563, 2001.
- [18] A. Crewe, F. Perrin, V. Benoit, K. Haddad, "Real-Time Pass-by Noise Source Identification Using a Beam-Forming Approach", SAE 2003 Noise & Vibration Conference and Exhibition, USA, 2003.

- [19] J. Affenzeller, A. Rust, "Road Traffic Noise – A Topic for Today and Future", VDA – Technical Congress 2005, Ingolstadt, Germany, 2005.
- [20] P. A. Morgan, P. M. Nelson, H. Steven, "Integrated assessment of Noise Reduction Measures in The Road Transport Sector", Project Report for European Commission, 2003.
- [21] S. Molla, E. Bongini, P. E. Gautier, D. Habault, P. O. Mattei, F. Poisson, "Vehicle Passby Noise Prediction and Audio Synthesis", 19th International Congress on Acoustics, Madrid, Spain, pp. 320-326, 2007.
- [22] K. Fujita, T. Abe, Y. Hori, "Simulation of Acceleration of Pass-by Noise Considering the Acoustic Radiation Characteristics of a Vehicle Body", J. Acoust. Soc. Am. 86, Vol:7, pp.52-58, 1986.
- [23] S.H. Park, Y.H. Kim, "Methods of Pass-by Noise Prediction in a Semi-anechoic Chamber," SAE Noise & Vibration Conference & Exposition, Traverse city, Michigan, USA, paper No: 971989, 1997.
- [24] S.H. Park, Y.H. Kim, "Visualization of pass-by noise by means of moving frame acoustic holography", J. Acoust. Soc. Am. Vol.110, No.5, pp2326–2339, November 2001.
- [25] S.H. Park, Y.H. Kim, "An improved moving frame acoustic holography for coherent bandlimited noise", J. Acoust. Soc. Am. Vol.104, No.6, pp340–348, December 1998.
- [26] A. Cerniglia, M. Lenti, "Noise sources investigation by beamforming method", ELPIT 2007, Togliatti, Russia, 2007.

- [27] L. C. Parra, "Steerable frequency-invariant beamforming for arbitrary arrays" *J. Acoust. Soc. Am.* 06, pp. 3839–3847, 2006.
- [28] R. A. Kennedy, T. Abhayapala, D. B. Ward and R. C. Williamson, "Nearfield broadband frequency invariant beamforming", *Proceedings of the Acoustics, Speech, and Signal Processing, Vol 2*, pp. 905-908, 1996.
- [29] F. Deblauwe, K. Janssens and B. Beguet, "A focalization technique to extend the usability of Near-Field Acoustic Holography and Beamforming", *Proceedings of Inter-Noise 07, Istanbul, Turkey*, p.07-128, 2007.
- [30] F. Deblauwe, K. Jansen, M. Robin, "Extending the usability of Near-Field Acoustic Holography and Beamforming by using Focalization", *14th International Congress on Sound and Vibration, Cairns, Australia*, p726, 2007.
- [31] H. Kook, G.B Moebs, P. Davies and J.S Bolton, "An Efficient Procedure For Visualizing The Sound Field Radiated By Vehicles During Standardized Passby Tests" *J. Sound Vib.* 233(1), 137–156, 2000.
- [32] Y.I. Wu, K.T. Wong, S. Lau, "Beacon-Aided Adaptive Localization of Sound Sources aboard a Pass-by Rail-car Using a Track-side Acoustic Microphone Array", *Proceedings of Inter Noise, Shanghai, China*, p0103, 2008.
- [33] M. Philip, K. U. Ingard, "Theoretical Acoustics in International Series in Pure and Applied Physics", McGraw-Hill, 1968.
- [34] Y.J. Kang, E.S. Hwang, "Beamforming-based Partial Field Decomposition in NAH" *J. Sound Vib*, pp. 867–884, 2008.

- [35] J. D. Maynard, "Acoustic Intensity from Holography: Introduction", Proceedings of Inter Noise 86, Cambridge, USA, pp. 1235-1240, 1986.
- [36] J. D. Maynard, E. G. Williams, and Y. Lee, "Near field acoustic holography: I. Theory of generalized holography and development of NAH," J. Acoust. Soc. Am, pp.1395–1413, 1985.
- [37] W. A. Veronesi, J. D. Maynard, "Nearfield Acoustic Holography (NAH): II. Holographic Reconstruction Algorithms and Computer Implementation", J. Acoust. Soc. Am. 81 (5), pp. 1307-1422, 1987.
- [38] P.R. Stepanishen, K.C Benjamin, "Forward and backward prediction of acoustic fields using FFT methods", J. Acoust. Soc. Am. 71, pp. 803-812, 1982.
- [39] E. G. Williams, B. H. Houston, P. C. Herdic, S. T. Raveendra, B. Garder, "Interior Near-Field Acoustical Holography in Flight", J. Acoust. Soc. Am. 108, Issue 4, pp. 1451–1463, 2000.
- [40] M. Nagamatsu, "Experimental Results of Converted NAH Method", JSME International Journal Series C, Vol. 49, pp. 670-674, 2006.
- [41] D. Vaucher, P. Chevret, F. Perrin, "Use of Acoustical Holography in 3D Interiors Measurements", Proceedings of Inter Noise 02, Dearborn, USA, pp. 1235-1240, 2002.
- [42] S. Dumbacher, J. Blough, D. Hallman, P. Wang, "Source Identification Using Acoustic Array Techniques" Proceedings of the SAE Noise and Vibration Conference, Traverse City, USA, Vol. 2, pp. 1023-1035, 1995.

- [43] M. D. Gardner, "Scan-Based Near-Field Acoustical Holography on Partially Correlated Sources", Master of Science Thesis, Brigham Young University, USA, 2009.
- [44] H. S. Kwon, Y. H. Kim, "Minimization of Bias Error due to Windows in Planar Acoustic Holography Using a Minimum Error Window", *J. Acoust. Soc. Am.* 98, Issue 4, pp. 2104–2111, 1995.
- [45] F. Jacobsen, G. Moreno, E. F. Grande, J. Hald, "Near Field Acoustic Holography with Microphones Mounted on a Rigid Sphere", *Proceedings of Inter-Noise 08*, Shanghai, China, p0495, 2008.
- [46] A. Fernandez, E. Silla, R. Soriano and R. Tormos, "Selective Near-Field Acoustic Holography", 19th International Congress on Acoustics, Madrid, Spain, sav-03-013, 2007.
- [47] Q. Wan and W. K. Jiang, "Near Field Acoustic Holography Theory for Cyclostationary Sound Field", 11th International Congress on Sound and Vibration, St. Petersburg, Russia, pp.3781-3787, 2004.
- [48] D. Hallman and J. S. Bolton, "Multi Reference Near field Acoustical Holography", *Proceedings of Inter Noise 92*, Toronto, Canada, pp. 1165-1170, 1992.
- [49] N. B. Roozen, W. Potze, E. Mulkens, "Nearfield Acoustic Holography Using Crossspectra" 9th International Congress on Sound and Vibration, Florida, USA, p. 221-5, 2002.
- [50] J. Hald, "STSF-a unique technique for scan-based Near-field Acoustical Holography without restrictions on coherence", *Brüel & Kjaer Technical Review No. 1*, 1989.

- [51] J. Hald, B. Ginn, "STSF in the Automotive Industry and Pass-by Noise Measurements", Brüel & Kjaer Technical Review No. 2, 1989.
- [52] J. Hald, B. Ginn, "Practical instrumentation and application", Brüel & Kjaer Technical Review No. 2, 1989.
- [53] K. Shin, J. Hammond, "Fundamentals of Signal Processing for Sound and Vibration Engineers", Wiley, First Edition, 2008.
- [54] W. C. Etten, "Introduction to Random Signals and Noise", Wiley, First Edition, 2005.
- [55] P. Kindt, D. Berckmans, F. DeConinck, P. Sas, W. Desmet, "Experimental Analysis of the Structure – Borne Tire/Road Noise due to Noise Discontinuities", Mechanical Systems and Signal Processing 23, pp. 2557-2574, 2009.
- [56] R. Bernhard, R. L. Wayson, "An Introduction to Tire/Pavement Noise of Asphalt Pavement", Quiet Pavement, www.quietpavement.com, Last visited on 13 July 2010.
- [57] S. F. Wu, Z. Zhou, "Simulation of Vehicle Pass-by Noise Radiation", Journal of Vibration and Acoustics, Volume 121, Issue 2, p.197, 1999.

APPENDIX A

Overview of the major changes to the test procedure in ISO 362-2007 (LMS DOCUMENT)

Adapting the testing method to vehicle performance:

The performance characteristics of the vehicle, be it a passenger vehicle, light truck or motorcycle, now play an important role in the testing process with the introduction of the Power to Mass Ratio (PMR) of the test vehicle.

$$PMR = \frac{P_n}{m_t} \times \frac{1000kg}{kWatt} \quad (A.1)$$

As its name suggests this is the ratio of the rated engine power, expressed in kW and the test mass of the vehicle. This mass that will be reported at the time of the test is made up of the kerb mass of the vehicle and the weight of the driver. The significance of the PMR, is that it defines the performance levels of the vehicle and consequently the parameters of the test procedure. A small European family car would have a PMR of about 45 whereas a sports car will have a PMR of around 150.

The Power to Mass Ratio determines the reference acceleration which is the target acceleration that the vehicle must achieve during the WOT

tests. Derived from statistical analyses, the reference acceleration is a logarithmic function of the PMR.

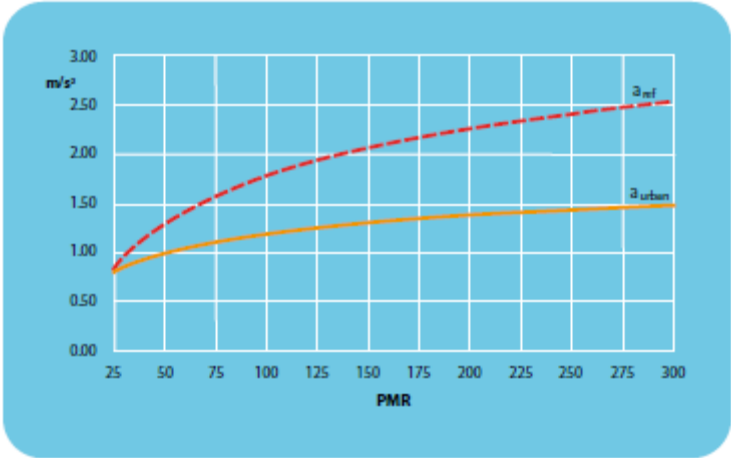


Figure A.1 Target acceleration (a_{ref}) for WOT tests and representative driving conditions for urban driving (a_{urban}) as function of PMR derived from statistical analysis

Selecting the test gears:

The selection of the gears that are taken into account for the calculation of the final PBN number, depends on how close the reference acceleration can be approximated during the WOT tests in each gear. For each gear, the actual test acceleration (a_{test}) is calculated using speed measurements at the start and end of the test zone averaged over four valid runs.

$$a_{test} = \frac{\left(\frac{V_{BB'}}{3.6}\right)^2 - \left(\frac{V_{AA'}}{3.6}\right)^2}{2 \times (20 + L)}$$

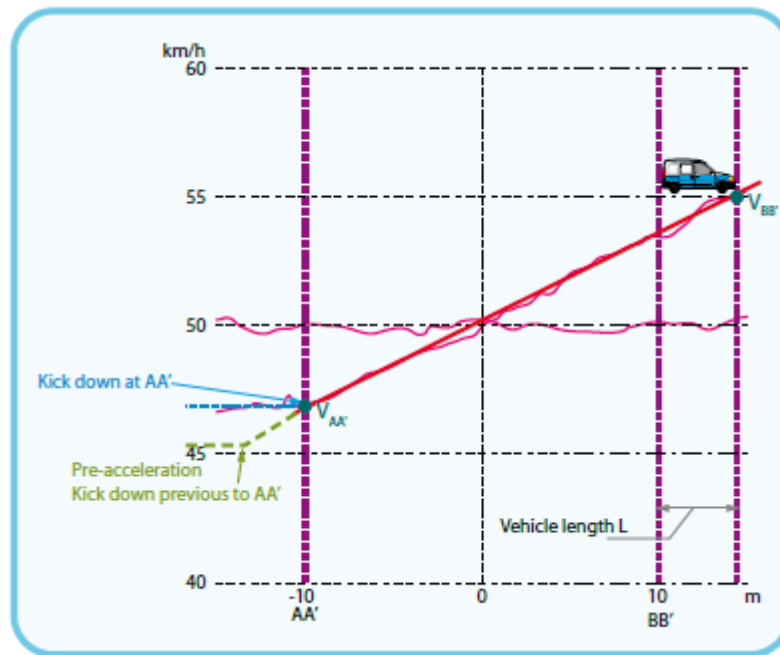


Figure A.2 Method to derive test acceleration from WOT test

If the test acceleration is within 5% of the reference acceleration (a_{ref}) then measurements need only be performed in a single gear. Gears for which the test acceleration is greater than $2m/s^2$ are rejected. Otherwise results are based on the combined results of test runs in two gears. This tends to make more use of 3rd and 4th gear, which is advantageous for powerful vehicles.

Where in the current ISO362 standard the vehicle must approach the point AA' of the test zone at 50 km/h, the draft standard requires the vehicle to reach 50 km/h at the moment it passes the microphones (PP'-line). This means that the approach speed has to be adapted depending on the actual WOT acceleration of the vehicle. The alternative is to apply a pre-acceleration. In this case the driver approaches the test zone at a fixed speed and goes full throttle before reaching the point AA'. In both cases it is not the easiest of goals to attain! Here an intelligent driver aid can overcome time-consuming trial and error work by the driver.

Constant speed tests as counterbalance for wide-open throttle:

Since the aim is to make the testing procedure more representative of urban driving and the noise problems associated with partial throttle acceleration, final results are weighted between wide-open throttle (WOT) measurements and constant road speed (CRS) measurements at 50 km/h. If two gears are required for the WOT tests, the constant road speed tests must also be performed in both gears.

The overall process to determine the final pass-by noise number is outlined in Figure 6.

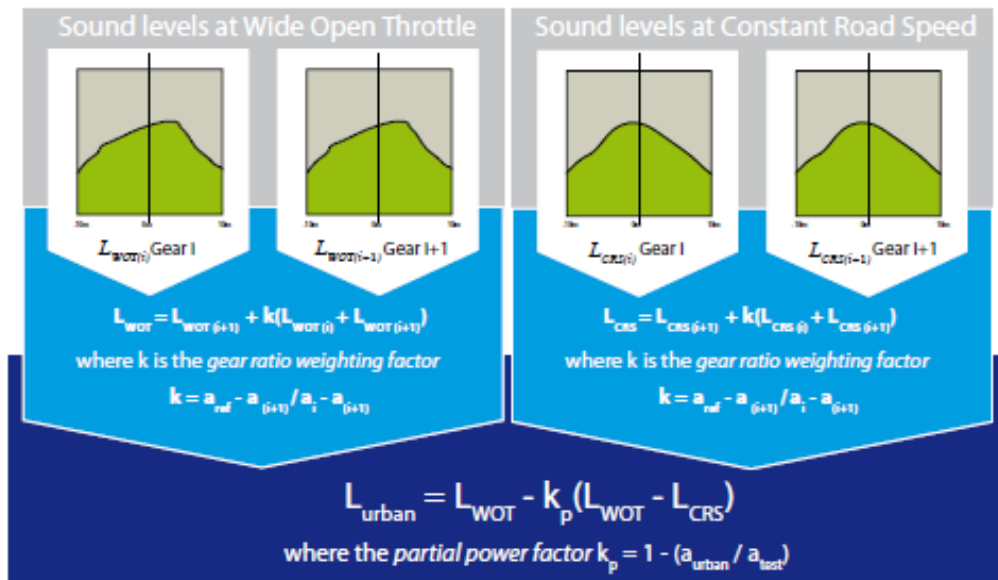


Figure A.3 Process to derive final PBN number L_{urban} by combining peak values of WOT and 50 km/h constant speed tests in two gears

A representative acceleration for urban traffic conditions a_{urban} was determined by statistical analyses to include 90% of noise levels of urban traffic. This target urban acceleration level is dependent on the PMR and can be seen in Figure A.3. Initial results indicate that for low PMR vehicles, resulting levels are slightly reduced. For high PMR vehicles more emphasis is

placed on the constant road speed test and the gears in which the tests are being performed are generally 3rd and 4th. For those vehicles to which this applies, this represents a significant difference.

Tighter test tolerances:

Although the accuracy requirements for the acoustic and meteorological measurements remain unchanged, engine and vehicle speed have to be measured more accurately. With the current standard 3% accuracy on both engine and vehicle speed were required. At 50 km/h this means 1.5 km/h while the draft standard imposes an accuracy of 0.2 km/h for vehicle speed measurements. Engine speed has to be measured with an accuracy of 2 %.

APPENDIX B

ROAD SURFACE REFLECTIONS

Road surface can play an important role in how the sound generated by the vehicle propagates. The effect of the reflection can be modeled as in the Figure B.1.

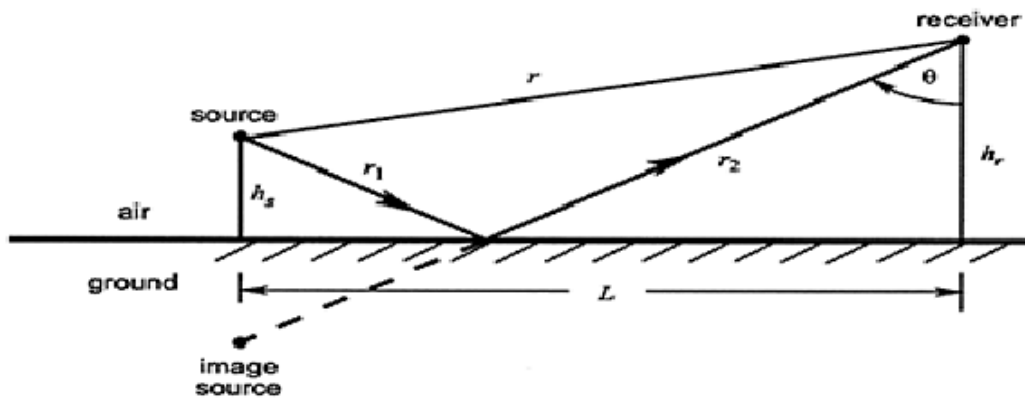


Figure B.1 Reflections on the Ground

In this mechanism, there are two waves radiated to the receiver point (K). If method of images is applied, sound pressure at the receiver point will be;

$$P_K = \frac{j\rho_0 ckQ_i}{4\pi(r_1 + r_2)} e^{j(\omega t - k(r_1 + r_2))} + \frac{j\rho_0 ckQ_s}{4\pi(r)} e^{j(\omega t - kr)} \quad (B.1)$$

If the surface of the road was perfectly reflective and rigid, then ($Q_s=Q_i$);

$$P_K = \frac{j\rho_o ck Q_s}{4\pi} e^{j\omega t} \left[\frac{e^{-jk(r_1+r_2)}}{(r_1+r_2)} + \frac{e^{-jkr}}{r} \right] \quad (B.2)$$

And if the receiver point (K) is moved to a coordinate where $r \approx r_1+r_2$, then;

$$P_K = \frac{j2\rho_o ck Q_s}{4\pi} e^{j(\omega t - kr)} \quad (B.3)$$

The meaning of this is that the sound pressure at the receiver point (K) is doubled in contrast to the case of no reflection. Also, this mechanism can be analyzed using a complicated formula which is based on empirical parameters and coefficients for characterizing the interaction between air and ground (asphalt) [12]. In this formula, road surface is characterized by its specific normal acoustic impedance " ζ " and according to the Delany and Bazley model for the reduced specific normal acoustic impedance, only the flow resistivity σ is needed to model the asphalt surface. The sound pressure at a point K is then;

$$P(K) \approx -\frac{e^{jkr}}{4\pi r} - (R_o + (1 - R_o)F) \frac{e^{jk(r_1+r_2)}}{4\pi(r_1+r_2)} \quad (B.4)$$

Where R_o is the plane wave reflection coefficient and F is a coefficient depending on specific normal acoustic impedance ζ .

APPENDIX C

ACOUSTICAL PREDICTION PROCESS

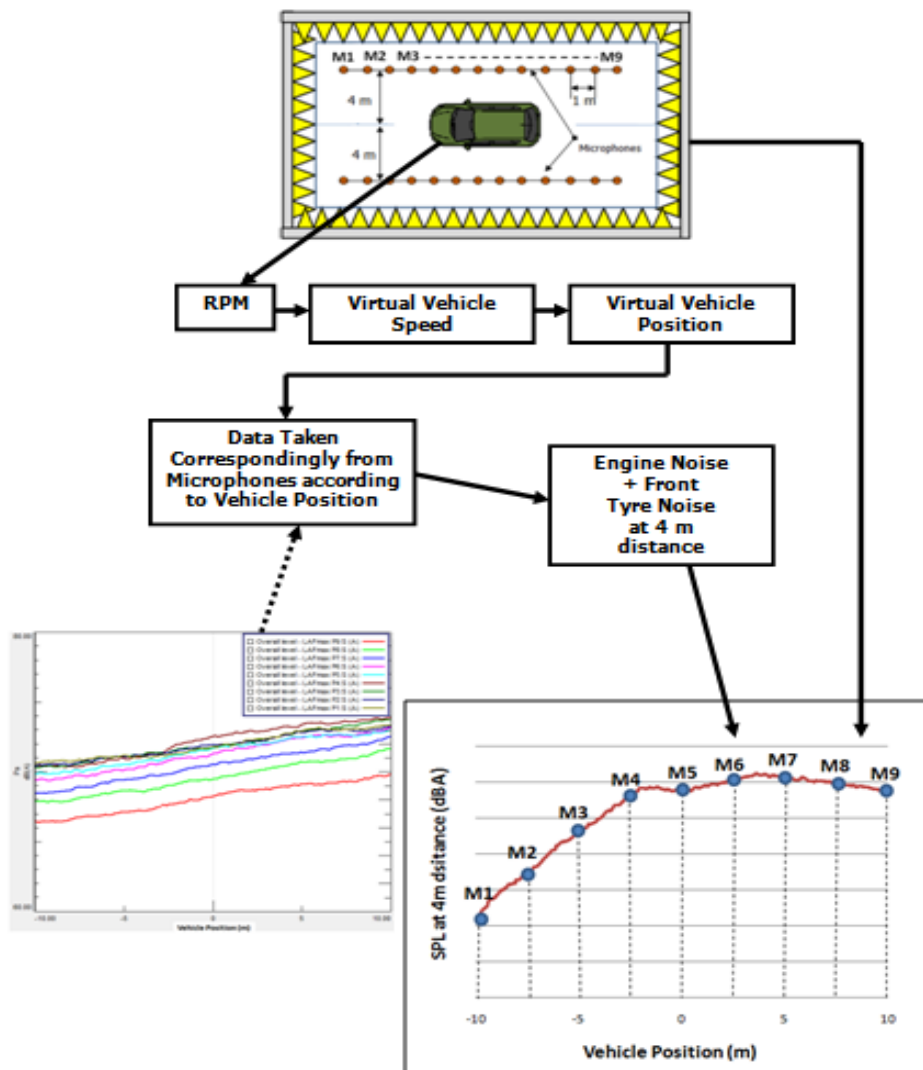


Figure C.1 First Stage of the Acoustical Prediction Process

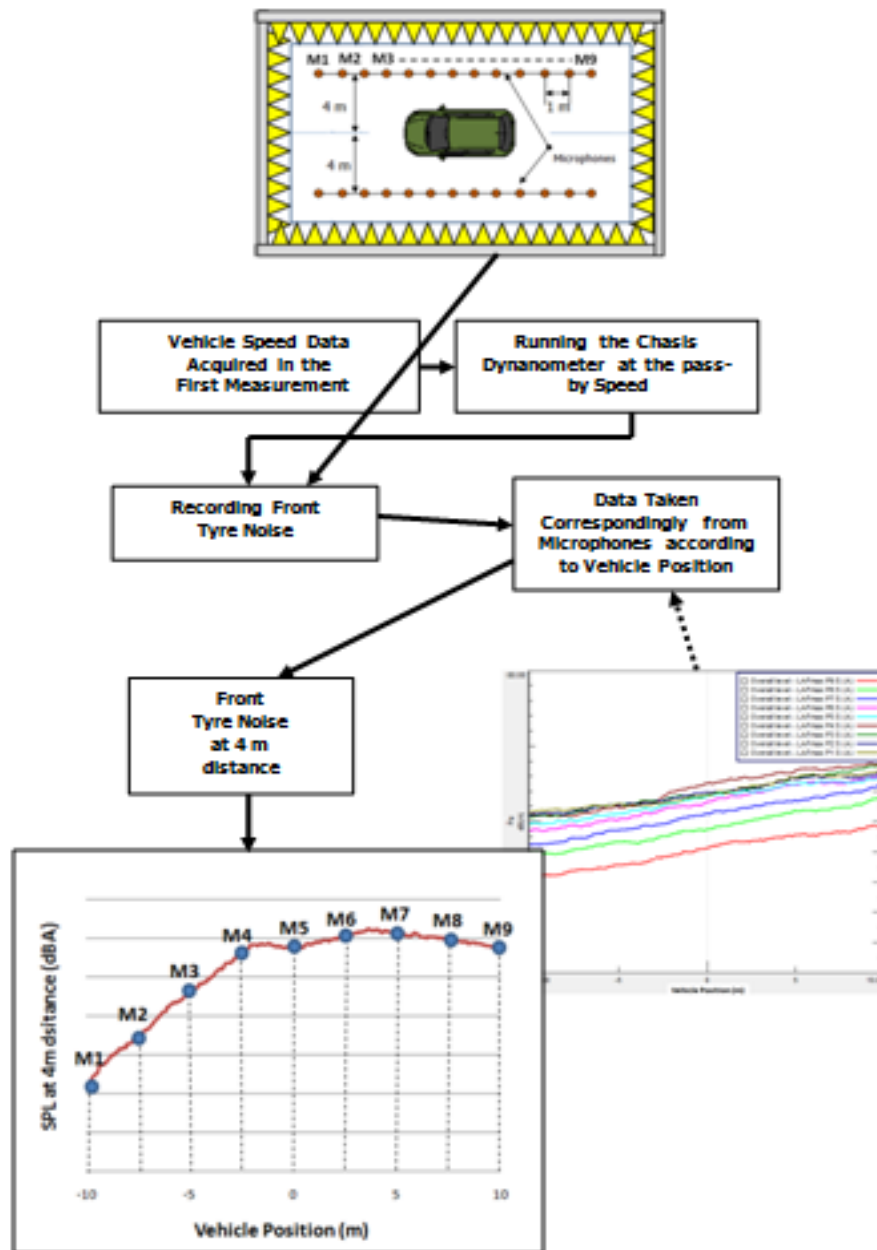


Figure C.2 Second Stage of the Acoustical Prediction Process

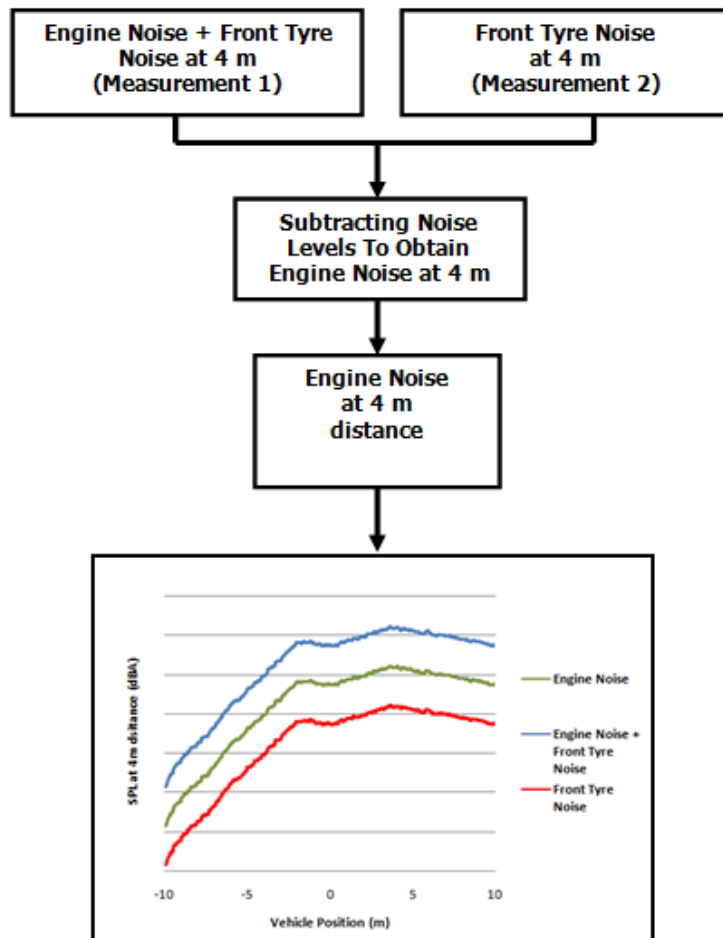


Figure C.3 Third Stage of the Acoustical Prediction Process

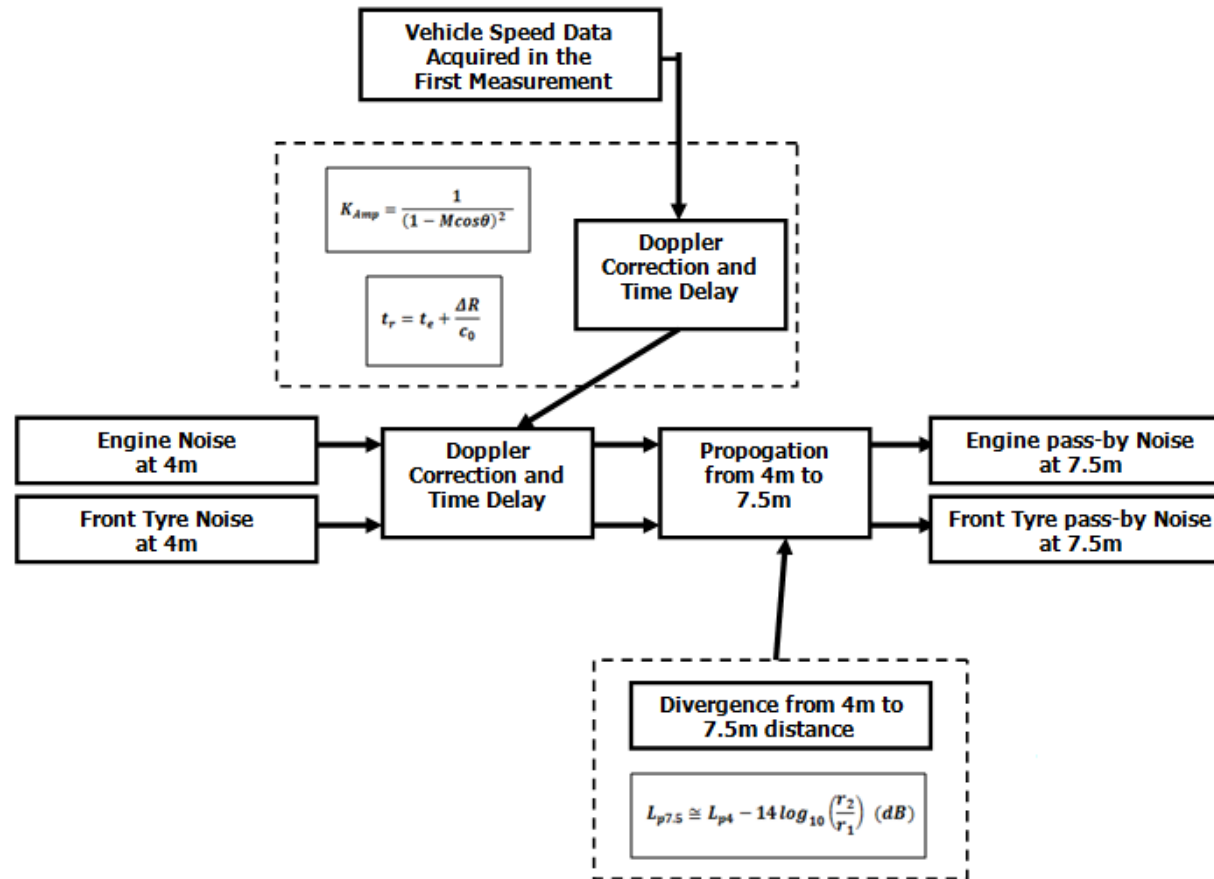


Figure C.4 Fourth Stage of the Acoustical Prediction Process

APPENDIX D

LMS SCADAS TECHNICAL PROPERTIES

LMS SCADAS Mobile at a glance

- 4 to 72 channels
- Master-slave configurations for distributed systems and channel expansion
- Up to 204.8 kHz sampling rate per channel
- 24-bit DSP technology
- 150 dB spurious-free dynamic range
- 8 Msamples/s throughput rate using high-speed Ethernet connection
- DC Automotive compliant (9-36V)
- Qualified for rough and high temperature operating conditions



SCM01

LMS SCADAS Mobile SCM01 mainframe: practical and ultra portable unit

- Accommodates 4 or 8 channels
- Compact, lightweight frame (203 x 58 x 260 mm/2.5kg)
- Nominal 2.5 hour battery autonomy
- On-board dual tachometer and generator
- Industry-standard Ethernet host interface
- On-board GPS receiver (optional) and CAN (optional)
- MIL-STD 810F qualified for shock and vibration



SCM05

LMS SCADAS Mobile SCM05 and SCM09 mainframes: optimal channel density in a small package

- Accommodates 4 to 40 channels (SCM05)
- Accommodates 4 to 72 channels (SCM09)
- Laptop-size robust frame (345 x 92 x 300mm (SCM05) 345x118 x300mm (SCM09))
- Nominal one-hour battery autonomy
- On-board dual tachometer and generator
- Industry-standard Ethernet host interface
- On-board GPS receiver (optional) and CAN (optional)
- MIL-STD 810F qualified for shock and vibration



SCM09

LMS SCADAS Mobile SCM06S and SCM10S slave frames

Expand mobile measurement to hundreds of input channels

- Accommodates 4 to 48 channels (SCM06S)
- Accommodates 4 to 80 channels (SCM10S)
- True master/slave configuration beyond clock synchronization: fully synchronized data is saved in one measurement file
- Easy mechanical locking of frames to 1 unit
- Distributed acquisition through 50m optical cabling